

NATURALISTIC DRIVING DATA FOR THE ANALYSIS OF CAR-FOLLOWING MODELS



**Morgan State University
The Pennsylvania State University
University of Maryland
University of Virginia
Virginia Polytechnic Institute & State University
West Virginia University**

**The Pennsylvania State University
The Thomas D. Larson Pennsylvania Transportation Institute
Transportation Research Building ❖ University Park, PA 16802-4710
Phone: 814-865-1891 ❖ Fax: 814-863-3707
www.mautc.psu.edu**

NATURALISTIC DRIVING DATA FOR THE ANALYSIS OF CAR-FOLLOWING MODELS

By: Hesham Rakha, John Sangster, and Jianhe Du

Mid-Atlantic University Transportation Center
Final Report

Department of Civil and Environment Engineering
Virginia Polytechnic Institute and State University

DISCLAIMER

The contents of this report reflect the views of the authors, who are responsible for the facts and the accuracy of the information presented herein. This document is disseminated under the sponsorship of the U.S. Department of Transportation's University Transportation Centers Program, in the interest of information exchange. The U.S. Government assumes no liability for the contents or use thereof.

February 21, 2013

1. Report No. VT-2010-01	2. Government Accession No.	3. Recipient's Catalog No.
4. Title and Subtitle Naturalistic Driving Data for the Analysis of Car-Following Models		5. Report Date February 21, 2013
		6. Performing Organization Code Virginia Tech
7. Author(s) Hesham Rakha, John Sangster, and Jianhe Du		8. Performing Organization Report No.
9. Performing Organization Name and Address Virginia Tech Transportation Institute 3500 Transportation Research Plaza Blacksburg, VA 24061		10. Work Unit No. (TRAIS)
		11. Contract or Grant No. DTRT07-G-0003
12. Sponsoring Agency Name and Address US Department of Transportation Research & Innovative Technology Admin UTC Program, RDT-30 1200 New Jersey Ave., SE Washington, DC 20590		13. Type of Report and Period Covered, Final Report
		14. Sponsoring Agency Code
15. Supplementary Notes		
16. Abstract This report presents two research efforts that have been published as conference papers through the Transportation Research Board Annual Meeting, the first of which is under review for journal publication. The first research effort investigates the general application of naturalistic driving data to the modeling of car-following behavior. The driver-specific data available from naturalistic driving studies provides a unique perspective from which to test and calibrate car-following models. As equipment and data storage costs continue to decline, the collection of data through in situ probe-type vehicles is likely to become more popular, and thus there is a need to assess the feasibility of these data for the modeling of driver car-following behavior. The first research effort seeks to focus on the costs and benefits of naturalistic data for use in mobility applications. Any project seeking to utilize naturalistic data should plan for a complex and potentially costly data reduction process to extract mobility data. A case study is provided using the database from the 100-Car Study, conducted by the Virginia Tech Transportation Institute. One thousand minutes worth of data comprised of over 2,000 car-following events recorded across eight drivers is compiled herein, from a section of multilane highway located near Washington, D.C. The collected event data is used to calibrate four different car-following models, and a comparative analysis of model performance is conducted. The results of model calibration are given in tabular format, displayed on the fundamental diagram, and shown with sample event charts of speed-vs.-time and headway-vs.-time. The authors demonstrate that the Rakha-Pasumarthy-Adjerid model performs best both in matching individual drivers and in matching aggregate results, when compared with the Gipps, Intelligent Driver, and Gaxis-Herman-Rothery models. The second effort examines how insights gained from naturalistic data may serve to improve existing car-following models. The research presented analyzes the simplified behavioral vehicle longitudinal motion model, currently implemented in the INTEGRATION software, known as the Rakha-Pasumarthy-Adjerid (RPA) model. This model utilizes a steady-state formulation along with two constraints, namely: acceleration and collision avoidance. An analysis of the model using the naturalistic driving data identified a deficiency in the model formulation, in that it predicts more conservative driving behavior compared to naturalistic driving. Much of the error in simulated car-following behavior occurs when a car-following event is initiated. As a vehicle enters the lane in front of a subject vehicle, the spacing between the two vehicles is often much shorter than is desired; the observed behavior is that, rather than the following vehicle decelerating aggressively, the following vehicle coasts until the desired headway/spacing is achieved. Consequently, the model is enhanced to reflect this empirically observed behavior. Finally, a quantitative and qualitative evaluation of the original and proposed model formulations demonstrates that the proposed modification significantly decreases the modeling error and produces car-following behavior that is consistent with empirically observed driver		

behavior.			
17. Key Words Traffic simulation, traffic modeling, driver behavior, car following		18. Distribution Statement	
19. Security Classif. (of this report)	20. Security Classif. (of this page)	21. No. of Pages 47	22. Price

Contents

NATURALISTIC DRIVING DATA FOR THE ANALYSIS OF CAR-FOLLOWING MODELS	1
ABSTRACT	7
INTRODUCTION	8
NATURALISTIC DRIVING DATA	8
Data Collection	8
Data Selection	9
Event Processing	9
Data Validation	11
Smoothing and Interpolating Data Elements	12
Summary of the Data Reduction Process	13
SUMMARY OF DATA ANALYZED	14
TRAFFIC SIMULATION CAR-FOLLOWING MODELS	16
Gaxis-Herman-Rothery (GHR) Model	16
Gipps Model	17
Intelligent Driver Model (IDM)	18
Rakha-Pasumarthi-Adjerid (RPA) Model	18
PARAMETER CALIBRATION	20
Discrete Time Generation of Vehicle Trajectories	20
Parameter Feasible Ranges	21
Optimization Functions to Match Simulated and Observed Results	21
RESULTS OF PARAMETER CALIBRATION	22
CONCLUSIONS AND RECOMMENDATIONS	27
ACKNOWLEDGEMENT	28
ABSTRACT	30
INTRODUCTION	30
DATASET	31
THE RAKHA-PASUMARTHY-ADJERID CAR-FOLLOWING MODEL	32
First-order Steady-state Car-following Model	32
Collision Avoidance Model	33
Vehicle Dynamics Model	34
PARAMETER CALIBRATION	34

Discrete Time Generation of Vehicle Trajectories	35
Parameter Calibration	35
Optimization Function	35
PARAMETER CALIBRATION RESULTS	35
First-Order Model Results	36
RPA Second-order Model Results	38
Empirical Observations of Driver Behavior	39
PROPOSED MODIFICATIONS TO THE MODEL	40
Use of Vehicle Dynamics for Coasting	41
Results of the Modified RPA Model	41
COMPARATIVE ANALYSIS FOR MODEL FORMULATIONS	43
Speed-spacing Area for Observed Data and Simulated Data	45
CONCLUSIONS.....	47
ACKNOWLEDGEMENT	48
REFERENCES	48

ABSTRACT

This report presents two research efforts that have been published as conference papers through the Transportation Research Board Annual Meeting, the first of which is under review for publication through the Transportation Research Record.

The first research effort investigates the general application of naturalistic driving data to the modeling of car-following behavior. The driver-specific data available from naturalistic driving studies provides a unique perspective from which to test and calibrate car-following models. As equipment and data storage costs continue to decline, the collection of data through in situ probe-type vehicles is likely to become more popular, and thus there is a need to assess the feasibility of these data for the modeling of driver car-following behavior. The first research effort seeks to focus on the costs and benefits of naturalistic data for use in mobility applications.

Any project seeking to utilize naturalistic data should plan for a complex and potentially costly data reduction process to extract mobility data. A case study is provided using the database from the 100-Car Study, conducted by the Virginia Tech Transportation Institute. One thousand minutes worth of data comprised of over 2,000 car-following events recorded across eight drivers is compiled herein, from a section of multilane highway located near Washington, D.C. The collected event data is used to calibrate four different car-following models, and a comparative analysis of model performance is conducted. The results of model calibration are given in tabular format, displayed on the fundamental diagram, and shown with sample event charts of speed-vs.-time and headway-vs.-time. The authors demonstrate that the Rakha-Pasumarthy-Adjerid model performs best both in matching individual drivers and in matching aggregate results, when compared with the Gipps, Intelligent Driver, and Gaxis-Herman-Rothery models.

The second effort examines how insights gained from naturalistic data may serve to improve existing car-following models. The research presented analyzes the simplified behavioral vehicle longitudinal motion model, currently implemented in the INTEGRATION software, known as the Rakha-Pasumarthy-Adjerid (RPA) model. This model utilizes a steady-state formulation along with two constraints, namely: acceleration and collision avoidance. An analysis of the model using the naturalistic driving data identified a deficiency in the model formulation, in that it predicts more conservative driving behavior compared to naturalistic driving. Much of the error in simulated car-following behavior occurs when a car-following event is initiated. As a vehicle enters the lane in front of a subject vehicle, the spacing between the two vehicles is often much shorter than is desired; the observed behavior is that, rather than the following vehicle decelerating aggressively, the following vehicle coasts until the desired headway/spacing is achieved. Consequently, the model is enhanced to reflect this empirically observed behavior. Finally, a quantitative and qualitative evaluation of the original and proposed model formulations demonstrates that the proposed modification significantly decreases the modeling error and produces car-following behavior that is consistent with empirically observed driver behavior.

Application of Naturalistic Driving Data to the Modeling of Driver Car-following Behavior

John Sangster, MS, PE

Center for Sustainable Mobility, Virginia Tech Transportation Institute
3500 Transportation Research Plaza
Blacksburg, VA 24061
Phone: (540) 231-1500
Email: johns80@vt.edu

Hesham Rakha, Ph.D., P.Eng. (corresponding author)

Charles E. Via, Jr. Department of Civil and Environmental Engineering
Center for Sustainable Mobility, Virginia Tech Transportation Institute
3500 Transportation Research Plaza
Blacksburg, VA 24061
Phone: (540) 231-1505
Fax: (540) 231-1555
Email: hrakha@vt.edu

Jianhe Du, Ph.D.

Center for Sustainable Mobility, Virginia Tech Transportation Institute
3500 Transportation Research Plaza
Blacksburg, VA 24061
Phone: (540) 231-1500
Email: jdu@vtti.vt.edu

ABSTRACT

The driver-specific data available from naturalistic driving studies provides a unique perspective from which to test and calibrate car-following models. As equipment and data storage costs continue to decline, the collection of data through in situ probe-type vehicles is likely to become more popular, and thus there is a need to assess the feasibility of these data for the modeling of driver car-following behavior. This paper seeks to focus on the costs and benefits of naturalistic data for use in mobility applications.

Any project seeking to utilize naturalistic data should plan for a complex and potentially costly data reduction process to extract mobility data. A case study is provided using the database from the 100-Car Study, conducted by the Virginia Tech Transportation Institute. One thousand minutes worth of data comprised of over 2,000 car-following events recorded across eight drivers is compiled herein, from a section of multilane highway located near Washington, D.C. The collected event data is used to calibrate four different car-following models, and a comparative analysis of model performance is conducted. The results of model calibration are given in tabular format, displayed on the fundamental diagram, and shown with sample event charts of speed-vs.-time and headway-vs.-time. The authors demonstrate that the Rakha-Pasumarthy-Adjerid model performs best both in matching individual drivers and in matching

aggregate results, when compared with the Gipps, Intelligent Driver, and Gaxis-Herman-Rothery models.

INTRODUCTION

Funding for large-scale naturalistic driving data studies has thus far been primarily for the purpose of conducting safety analysis, with application of the dataset in a mobility context done as a secondary objective. Data collected in a naturalistic way for safety studies can provide significant information including: detailed pre-crash/crash information; measures of driver distraction or drowsiness; instances of aggressive driving or driver error; and the incorporation of vehicle dynamics. Similar advantages can be found in the application of these data in the context of mobility applications, where naturalistic data are able to provide detailed driver information, while also providing real-world driving data with a minimal amount of bias.

This paper seeks to examine the procedure of processing a large-scale naturalistic database for mobility analysis, specifically with application to the calibration of car-following models. In order to validate a given car-following model, observations must be made of lead-follower vehicle pairs, with comparisons made between the simulated follower and the observed follower behavior. The data used to validate car-following models in the past has primarily come from test tracks, simulators, or loop detectors. These studies either have driver-specific information and bias from lack of real-world driving situations, or accurate real-world driving data from anonymous drivers. Only recently has naturalistic driving data become available as an analysis data source [1].

There are many explanations of the importance of car-following models in microscopic traffic-simulation in the literature, with an informative and succinct example being that of Panwai and Dia [2], who explain that traffic-simulation tools provide the ability to evaluate and control different scenarios in an environment that doesn't disrupt real-world traffic conditions. The data available from naturalistic driving behavior studies can provide unique insight into the quality of car-following models, particularly in their ability to accommodate diverse individual drivers.

NATURALISTIC DRIVING DATA

A natural consequence of the proliferation in cell-phone and computing power will be an increasing availability of naturalistic driving data, and it is essential for researchers to understand the complications of working with such large datasets. The large size of the database generated by a naturalistic driving study requires data reduction to be conducted using a carefully planned procedure. In the case of the 100-Car Study, the initial dataset includes 108 individual drivers, with nearly 337,000 hours of data collected across 207,000 trips, which results in more than 12 billion database observations using a sampling frequency of 10 Hertz (i.e. data gathering every 0.1 seconds). The data analyzed herein are identified using a geographic information system (GIS) application to visually select specific routes and drivers, exporting pertinent data to define trips of interest. Data validation is conducted on the selected data by examining outlier information. Some post-processing is necessary in cases where information is updated less often than is sampled.

Data Collection

Within the naturalistic driving study, each of the sensing subsystems within the vehicle is kept independent of the others in order to constrain failures to a single sensor type [3]. Sensors may include: a box to obtain data from the vehicle network on-board diagnostic (OBD) system; an

accelerometer box for longitudinal and lateral acceleration measurement; a system to provide information on the spacing between the lead and following vehicles; a system to detect conflicts with vehicles in adjacent lanes; an incident box to allow drivers to flag incidents for the research team; a video-based lane tracking system to measure lane keeping behavior; and video feeds for validation of other sensor data. The video feed may include multiple camera views monitoring the driver's face and the driver's side view of the road, the forward road view, the rear road view, the passenger side view of the road, and a view of the driver's hands. Captured video data are synchronized with the other sensor data to allow simultaneous display of archived information. A global positioning system (GPS) is used to collect information on the vehicle position.

Management of the data in a naturalistic driving study is of primary importance in order to ensure that the data gathered are accessible and secured, maximizing their utility. These datasets may contain billions of time-steps worth of data, and are generally managed through relational databases.

Data Selection

Through an SQL program application, database information are selected and saved as separate files differentiated by driver ID, with these files imported to a GIS application using the stored GPS data. Regular commuting routes for each driver are identified where possible, maintaining a tabular list of all drivers and their corresponding commonly traveled routes. In this way specific routes regularly traveled by multiple drivers are identified. It is essential to extract data for each driver for the identical roadway segment in order to isolate and characterize differences in driver behavior. In the case of the 100-Car study, it was found that multiple drivers traverse the Dulles Airport Access Road (DAAR) on a regular basis. Fifteen drivers identified through the GIS visual review yields a total of more than 500 hours' of data, just over one percent of the total database.

Event Processing

With specific drivers and routes identified through visual inspection, a preliminary data subset is identified of all data points along the given route belonging to drivers who frequently use the route. This data not only includes all data points travelling within a certain radius of this route, and must be further analyzed to identify specific lead-follower vehicle pairs which may represent car-following events. A sample process designed for application to the 100-Car Study is seen in **FIGURE 1**, which may have application to other naturalistic data sets.

Researchers wishing to investigate car-following behavior using naturalistic databases should not take the process diagram to be proscriptive, because other study databases are likely to be organized differently than was the 100 Car Study database. The process begins with the subset of data selected using GIS, labeled as D***_DAAR. Because an offset area method was used in GIS to select data, points beyond the limit of the study area were included in the subset of data, and were removed using a spreadsheet application by examining longitude information. The pertinent data elements were then merged using an SQL application with the corresponding radar information, resulting in D***_DAAR_RAD. Lead-follower pairs were generated from the radar information, and verified using the forward-facing video feed, resulting in D***_DAAR_EVNT. Because the lead vehicle is often incorrectly renumbered partway through an event by the radar equipment, the D***_DAAR_EVTS file identifies the manually identified begin and end frame for an event, as well as the number associated with the lead vehicle over the course of the event. The various datasets stored in the database are then merged using the event

information to generate the final file used for analysis, D***_DAAR_USE. In all cases the *** in the file name refers to the individual driver number.

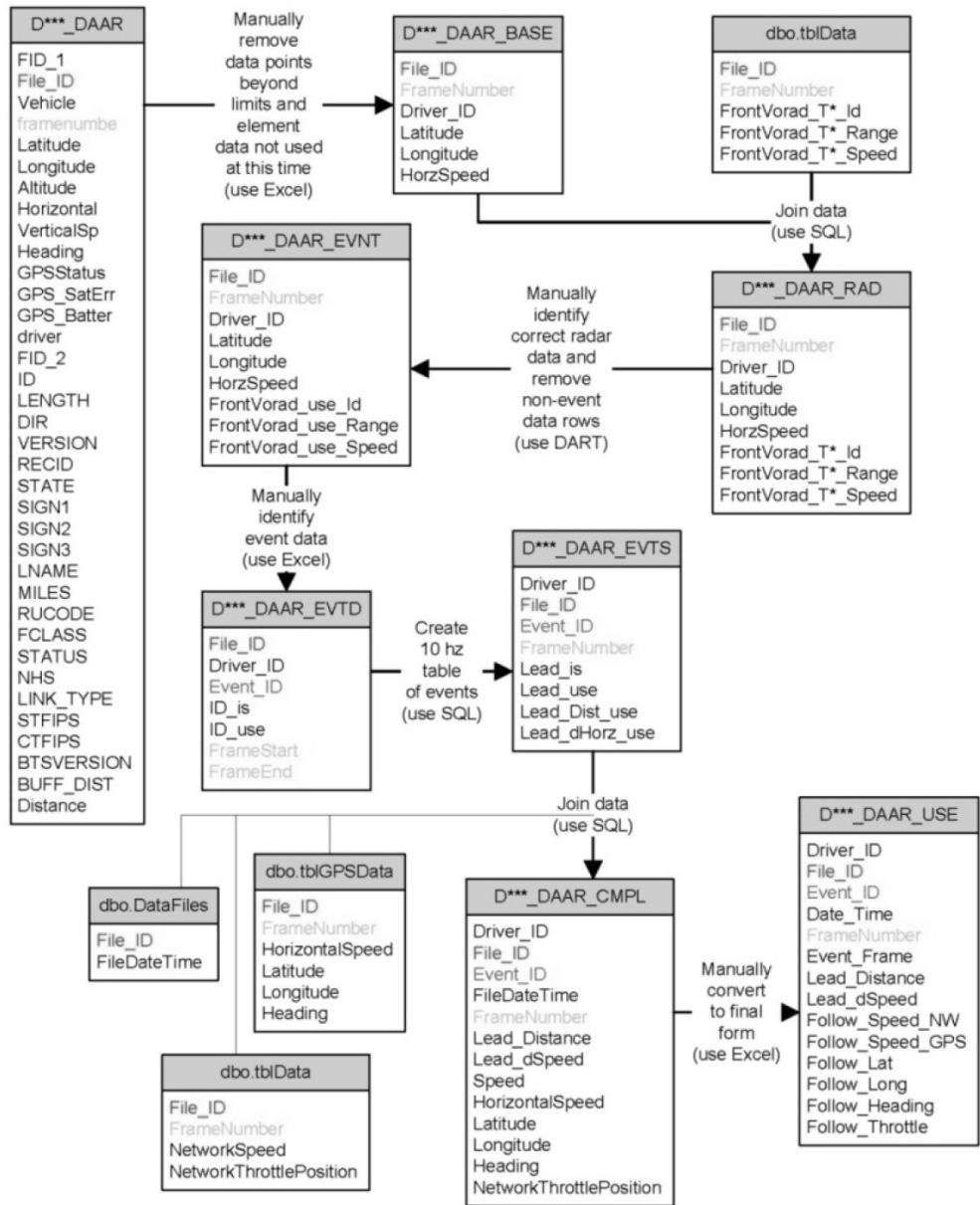


FIGURE 1 Process diagram for generation of car-following data from selected GIS data.

The forward facing radar used in the 100-Car Study tracks up to seven individual objects at a time, assigning identification numbers sequentially from 1 to 255 as each new object is observed. In reviewing the radar data it was concluded that the technology is not reliable for the purpose of systematically identifying car-following events. Errors observed with the radar equipment include: many vehicles are seen on the video but are not found by the radar; a vehicle being tracked by the radar is sometimes lost if the speed of that vehicle matches the speed of the probe vehicle; periodically the radar appears to experience a technical hiccup, with all tracked vehicles being lost, and new identification numbers assigned as they are re-acquired. Data noise generated

by the radar system is overcome by conducting manual review of potential car-following events, corroborating the forward-facing video with the radar data, as seen in **FIGURE 2**. The gray panel on the right displays the vehicles being tracked by the radar both in front and behind the vehicle, and is tied by data frame number to the video feeds displayed in the center of the screen. The top left video feed displays the driver's face and the area adjacent to the vehicle on the driver's side, and has been blanked out herein for privacy reasons.

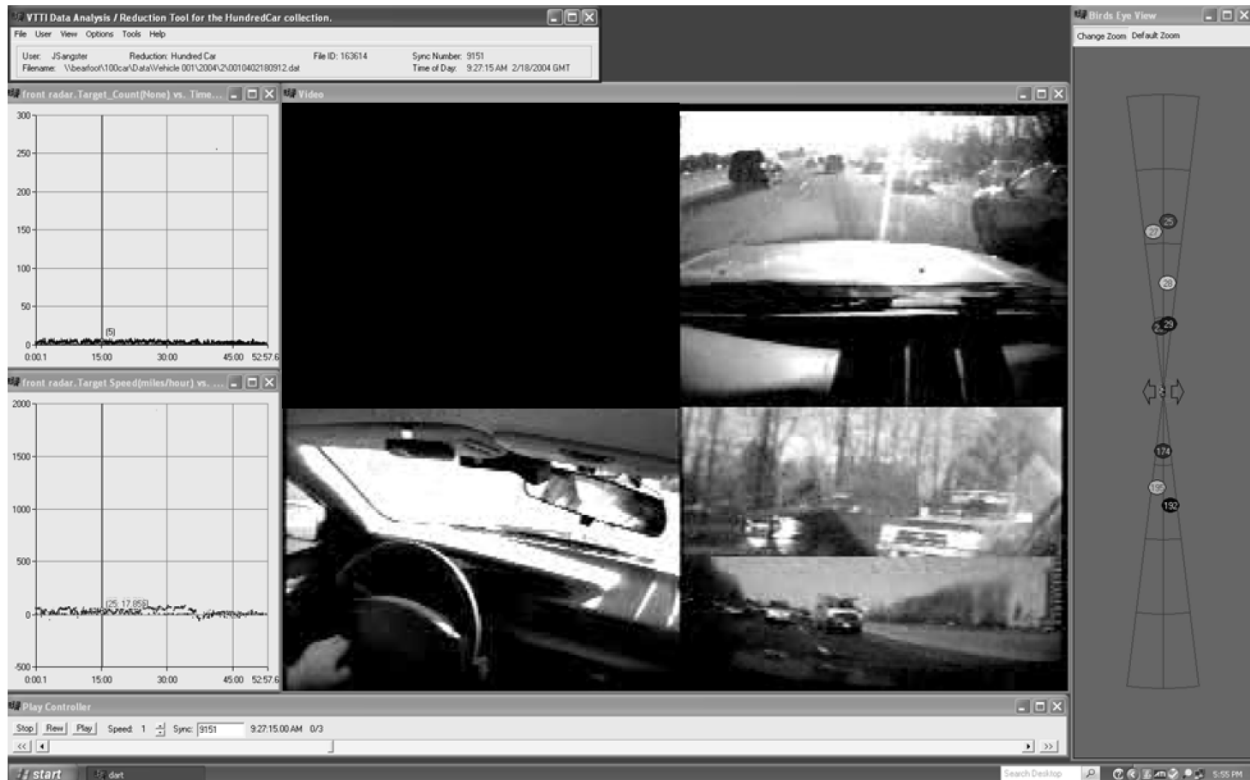


FIGURE 2 Example of visualization for data reduction.

In addition to problems with the radar equipment, much of the identified data along the DAAR corridor experienced occlusion of the forward facing video feed for a variety of reasons, including: a lack of contrast during nighttime driving; the blurring of the view from rain precipitation; a covered view due to the build-up of frozen precipitation; and a lack of contrast due to glare at sunrise or sunset. The video feed is not the only system to experience data outages, with one estimate from the 100-Car Study indicating that 1.37 million miles of data are complete out of an estimated total of 1.80 million miles of possible data, resulting in a 24% loss of data due to major or minor failures in hardware and/or software [3]. For the dataset identified through the visual process using GIS, seven of the identified drivers exhibited a failure of the video, radar, or speed recording devices, resulting in only eight of the fifteen identified drivers generating usable data.

Data Validation

The speed of the follower vehicle is obtained from either the OBD or from an interpolation of the recorded geospatial coordinates. In the case of the 100-car study, both sources of speed data update their internal values at a frequency of one second, while the database retrieves and stores

the values at a frequency of one tenth of a second; in practice, this results in ten time-steps worth of data showing the same value, updated instantaneously to a new value, with the new value then held for ten time-steps. The OBD data was found to be more reliable than the GPS speed data; the spatial coordinates of a moving object in GPS are seen to have a tendency to lag and then catch up, resulting in a recorded speed that oscillates, sometimes greatly, about the actual speed traveled by the vehicle. The follower speed generated by the GPS is used as a check of the OBD speed, which itself regularly experiences faults with incorrect data or no data recorded.

The radar data is an essential component of the naturalistic data for mobility applications, but is not as essential in conducting safety studies, so it may consequently suffer from either dependability or accuracy issues. The radar generally exhibits a capture area that is cone shaped, tracking multiple objects within the cone by assigning object identification numbers to each object as it is first acquired. If an object's speed exactly matches that of the instrumented vehicle, it has a tendency to drop from the radar data, being assigned a new identification number as it is reacquired. For the data analyzed herein visual confirmation was conducted for each event, and in cases where a lead vehicle is assigned more than one identification number in the dataset, the value was manually overridden with the original vehicle identification number.

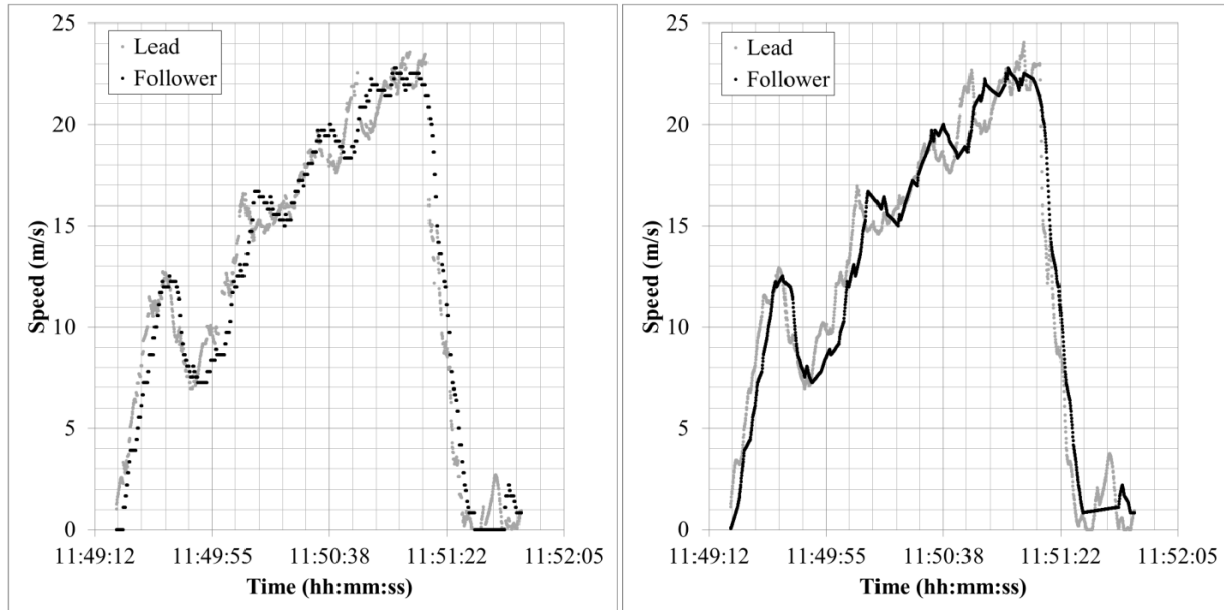
Smoothing and Interpolating Data Elements

When examining the OBD speed data it is seen that the recorded value will sometimes become fixed for short periods of time (a few seconds) at a given value before being updated with the correct information. The value is understood to be erroneous due both to changes in the recorded GPS speed values and due to the magnitude of the instantaneous acceleration observed when the value does eventually update. For this, and other reasons, outlier data are observed in the raw data obtained through the GIS application. Outlier data are identified within the dataset by checking the observed speed and acceleration values against the physical limitations of speed and acceleration anticipated knowing the vehicle characteristics. The outlier data are replaced with interpolated data using linear interpolation between two of the observed values considered to be valid, with a maximum length of interpolated data being two seconds.

As a result, the dataset resulting after validation is a somewhat of a truncated version of the raw data. For example, the 99.9th percentile probe vehicle velocity observed in the raw data is 40.10 m/s before validation and smoothing, and 32.04 m/s after. The maximum probe vehicle instantaneous acceleration and deceleration observed before smoothing is 303.0 m/s², and 303.6 m/s², respectively. With smoothing the maximum deceleration rate is 9.012 m/s², and the maximum acceleration rate is 8.893 m/s², respectively. While the smoothed values are still beyond the physical limitations of the vehicles, they are representative of the step-wise accuracy of the recorded velocity.

In order to provide vehicle trajectory profiles for analysis, the frequency with which values are updated is made equal to the frequency with which the data are analyzed. To update the raw OBD speed data, updated on average every second, the observed value is maintained whenever it varies from the previous time step, and the data is removed whenever the value remains constant to the previous time step value; the missing data is then refilled using linear interpolation, so long as the gap between observed values does not exceed two seconds, in which case the event is split into two separate events on either side of the data gap. Because a number of car-following models require an offset time, only events longer than five seconds in duration, 51 time-steps or greater, were used in the analysis. This interpolation of data elements serves as a final validation of the lead-follower pairs, identifying any errors occurring during the previous data reduction

steps. An example of how the interpolation of data elements affects vehicle speed trajectories is seen in **FIGURE 3**.



(a) Speed vs. time without interpolation **(b) Speed vs. time after interpolation**
FIGURE 3 Effect of interpolation on sample lead and follower vehicle speed profiles.

Summary of the Data Reduction Process

The procedure outlined herein is applicable to conducting data reduction for any naturalistic driving database, and is intended for use by others in planning future research. A first step in selecting a subset of data for analysis is the use of a GIS application to identify frequently traveled routes, in order to generate a significant number of car-following events on a given facility. With a subset of the total travel data selected, car-following events must be identified from the database; the complexity of this step may vary depending on how many travel lanes there are on the facility selected. In the example provided herein, events were validated by corroborating the radar feeds with forward-facing video.

Future research projects can expect to encounter complications with data validation when using naturalistic driving data. The case study herein observed that equipment recording video, speed, and radar information all experienced regular failures; as a result only half of the original data identified from the dataset was valid for analysis. Future studies should anticipate these types of equipment failures during the data collection process. Additionally, it was found that the data values stored by the equipment were updated less frequently than they were reported, requiring the development of an interpolation and smoothing process to impute missing data and smooth the data.

SUMMARY OF DATA ANALYZED

A tabular summary of the data analyzed for this study is seen in **TABLE 1**. Note that seven of the initially identified fifteen drivers are missing data critical for the identification of car-following events, resulting in a total dataset of 1,000 minutes of car-following data from the initial 30,213 minutes of data identified in the GIS tool.

TABLE 1 Quantity of data included herein

	Driver	Raw Data	Car-Following Pairings	
	Number	Minutes	Events	Minutes
Valid Data	124	636	188	80
	304	1,424	149	69
	316	4,280	332	191
	350	1,797	274	62
	358	1,712	443	186
	363	2,854	274	176
	367	2,991	507	211
	462	813	72	25
Invalid Data	102	152	Not Enough Leader-Follower Data	
	351	2,431	Missing Video or Speed Data	
	359	2,921	Missing Video or Speed Data	
	402	2,171	Missing Video or Speed Data	
	409	5,228	Missing Video or Speed Data	
	452	228	Missing Video or Speed Data	
	461	576	Missing Video or Speed Data	
	Total	30,213	2,239	1,000

The macroscopic diagram provides a visual context to analyze and compare driver behavior from a naturalistic driving behavior study, such as seen in **FIGURE 4**.

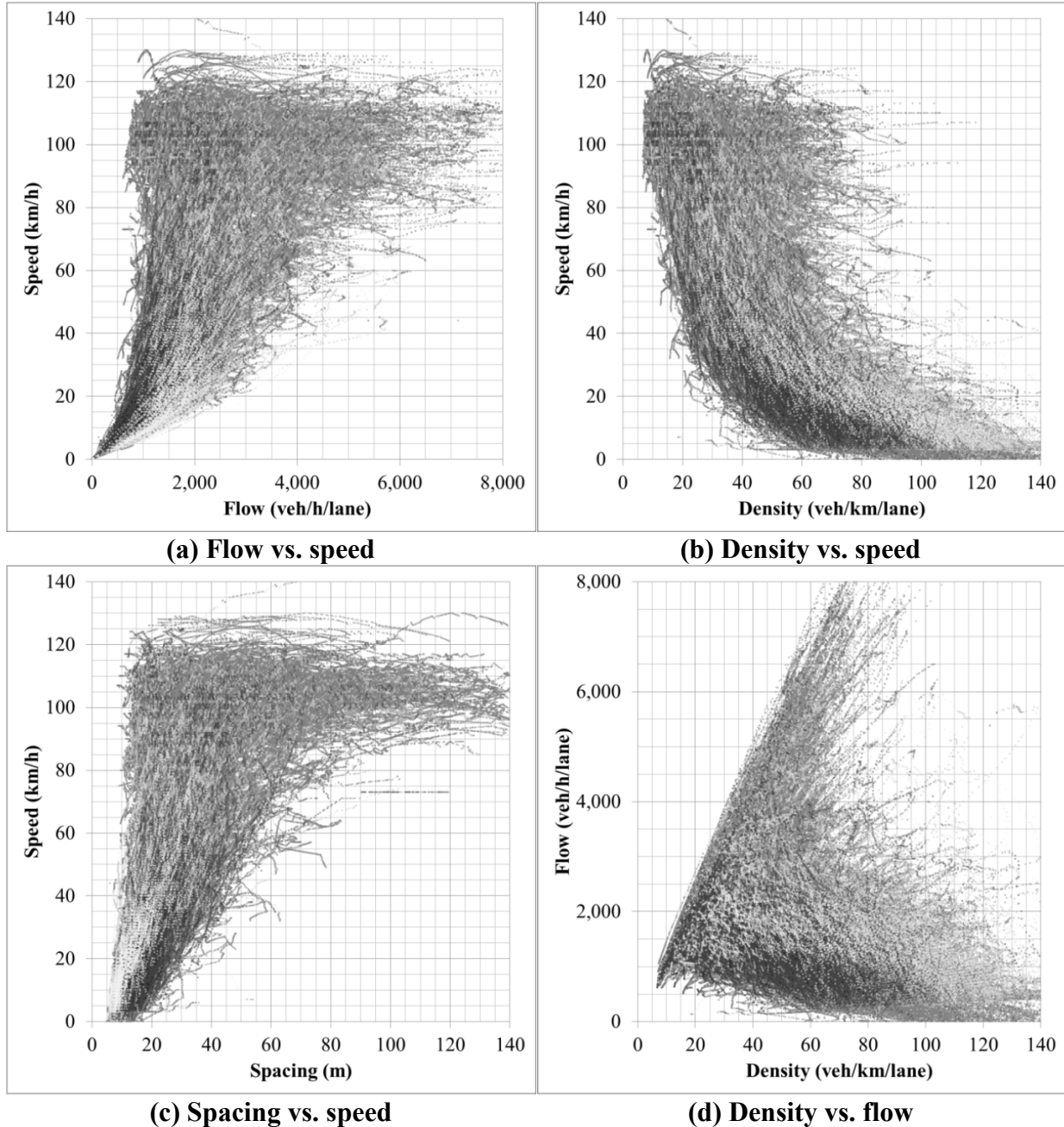


FIGURE 4 Combined fundamental diagram for car-following event data; displaying (a) flow vs. speed, (b) density vs. speed, (c) spacing vs. speed, and (d) density vs. flow.

The data from the eight drivers is aggregated into four views of the fundamental interaction diagram, with grayscale used to indicate steady-state conditions separately from acceleration and deceleration regimes. The darkness of the data points indicates the magnitude of acceleration, with near-black points indicating high acceleration, and near-white points indicating high deceleration. The interaction diagram will serve as a primary format for visualizing the results of simulated car-following models, as well as analyzing other areas of interest related to driver behavior.

TRAFFIC SIMULATION CAR-FOLLOWING MODELS

Each car-following model predicts the time-space trajectory of a following vehicle when provided the time-space trajectory of a leading vehicle, along with the original location and velocity of the following vehicle. The parameters of each model are calibrated such that the resulting simulated behavior matches the observed behavior as closely as possible. In calibrating the model parameters it is necessary to define limiting bounds for the parameter values, define an error function, select an optimization methodology to minimize the objective function, and generate observed and simulated vehicle trajectories.

As presented in this paper, the car-following models share a common notation, which includes:

n	=	<i>vehicle number n: the leading vehicle</i>
$n + 1$	=	<i>vehicle number $n + 1$: the following vehicle</i>
x, \dot{x}, \ddot{x}	=	<i>vehicle position, velocity, and acceleration, respectively</i>
\ddot{x}_{d-max}	=	<i>maximum acceleration rate desired by driver of vehicle $n + 1$</i>
\ddot{x}_{d-min}	=	<i>maximum deceleration rate desired by driver of vehicle $n + 1$</i>
\dot{x}_d	=	<i>velocity desired by driver of vehicle $n + 1$</i>
Δ	=	<i>the change in value for a given variable at a given time step between the leading and following vehicle</i>
Δx_j	=	<i>vehicle spacing at standstill (i.e. jam density spacing)</i>
t	=	<i>the current time step</i>
τ	=	<i>the perception reaction time</i>

An example of the notation is:

$$\Delta \dot{x}_{n \rightarrow n+1}(t - \tau) = \text{the change in velocity between the leading and following vehicle that occurred at the } (t - \tau) \text{ time-step.}$$

Gaxis-Herman-Rothery (GHR) Model

The GHR type of model, also known as the GM model, involves research spanning from the late 1950's until the mid-1960's [4], [5]. A discussion on the development of the General Motors models along with typical parameter values can be found in May [6], among others. The fifth and final formulation of the model, sometimes referred to as the GM-5 model, generalizes the previous four forms and is seen in Equation (1).

$$\ddot{x}_{n+1}(t) = \left\{ \frac{\alpha [\dot{x}_{n+1}(t)]^z}{[\Delta x_{n \rightarrow n+1}(t - \tau)]^l} \right\} \cdot [\Delta \dot{x}_{n \rightarrow n+1}(t - \tau)] \quad (1)$$

Where: $\alpha, z, l =$ model parameters that require alibration

The GHR model is particularly significant in the pantheon of car-following models as many other microscopic and macroscopic models can be represented as special cases of the GHR model. The first single-regime traffic stream model proposed by Greenshields in 1935 is one such case [7]. It can be expressed as a GHR model taking the z and l parameters to be 0 and 2, respectively. The CORSIM transportation simulation software operates based on the PITT model, which has been shown to be analogous to the Pipes car-following model [8–10]. In turn, the formulation of the Pipes model can be seen to be a special case of the GHR model with the z and l parameters set to zero.

As the other models analyzed herein are representative of higher order models, the GM-5 formulation of the GHR models will be used in the analysis portion of this paper. Additionally, in line with previously documented calibration procedures for the GM-5 car-following model,

the z and l parameters will be calibrated separately under acceleration and deceleration conditions, which provides a like number of calibration parameters among the models analyzed herein [11].

When simulating the GHR model for this study additional constraints are added to the calculations; the simulated velocity is held at a minimum of 0.1 m/s, and the simulated position offset is held at a minimum of 5 meters behind the leading vehicle.

Gipps Model

First published in 1981, Gipps developed a model as a response to the existing proliferation of GHR type models [12]. The model seeks to: mimic the behavior of real traffic; use parameters that correspond to characteristics of drivers and vehicles so that most can be assigned without calibration procedures; and provide reasonable results if the interval of speed and position calculations is similar to that of the reaction time. The model takes the form of Equation (2).

$$\dot{x}_{n+1}(t) = \min \text{ of:}$$

$$\dot{x}_{n+1}(t - \tau) + 2.5\ddot{x}_{d-max} \cdot \Delta t \cdot \left[1 - \frac{\dot{x}_{n+1}(t-\tau)}{\dot{x}_d}\right] \cdot \sqrt{0.025 + \frac{\dot{x}_{n+1}(t-\tau)}{\dot{x}_d}},$$

$$\ddot{x}_{d-min} \cdot \Delta t + \sqrt{\left(\ddot{x}_{d-min}^2 \cdot (\Delta t)^2 - \ddot{x}_{d-min} \cdot \left\{2[\Delta x_{n \rightarrow n+1}(t - \tau) - \Delta x_j] - \left[\dot{x}_{n+1}(t - \tau) \cdot \Delta t\right] - \frac{\dot{x}_n(t-\tau)^2}{\dot{x}_{(n)-min}}\right\}\right)} \quad (2)$$

$$\text{Where: } \ddot{x}_{(n)-min} = \min\left(-3.0 \text{ m/s}^2, \frac{\ddot{x}_{d-min} - 3.0}{2}\right)$$

the estimate made by the driver of vehicle $n + 1$ of the maximum deceleration rate desired by the driver of vehicle n

The first component of the two-regime equation applies to traffic conditions with unconstrained flow, also known as steady-state flow conditions. The second component addresses conditions in constrained flow, where the velocity of the follower vehicle is based primarily on the time/space headway the must necessarily maintain a safe distance between it and the lead vehicle. Since the original publication of the Gipps' model, a number of publications examining the calibration of the Gipps model have brought up critique in two areas: the feasible range for the expected maximum deceleration of the leading vehicle; and the relationship between the perception-reaction time and the time-step [13–15].

Wilson primarily examined the wave-stability of the Gipps model, and specifically looked at cases where $\ddot{x}_{d-min} > \ddot{x}_{d-min,n}$ or $\ddot{x}_{d-min} < \ddot{x}_{d-min,n}$ [13]. Wilson determined that in some cases that the anticipated deceleration of the leading vehicle is expected to be less than the desired maximum deceleration of the following vehicle, the resulting time-space wave phenomenon becomes unstable. If the original formulation of the Gipps model is used, the implication would be that any follower vehicle with a desired deceleration in excess of -3.0 m/s^2 would fall into the category of potentially being infeasible. For the purposes of the model calibration performed herein, Gipps' original formulation for the anticipated leading vehicle maximum deceleration is used.

Rakha *et. al.*, building on the work of Wilson, developed a method to express the steady-state portion of the Gipps model on the macroscopic fundamental diagram [14], [15]. The speed-flow relationship can be computed using Equation (3), and subsequently, the perception-reaction time can be computed using Equation (4).

$$q = \frac{1,000 * \dot{x}_{n+1}}{\Delta x_j + \frac{1}{2.4} * \tau * \dot{x}_{n+1} + \frac{1}{25.92 * \ddot{x}_{d-min}} * \left(1 - \frac{\ddot{x}_{d-min}}{\ddot{x}_{d-min,n}}\right) * \dot{x}_{n+1}^2} \quad (3)$$

$$\tau_m = 2.4 \left(\frac{1,000}{q_c} - \frac{\Delta x_j}{\dot{x}_{capacity}} - \frac{\dot{x}_c}{25.92 * \ddot{x}_{d-min}} \left(1 - \frac{\ddot{x}_{d-min}}{\ddot{x}_{d-min,n}}\right) \right) \quad (4)$$

Where: q = flow rate (veh/hr/ln)
 q_c = flow rate at capacity (veh/hr/ln)
 \dot{x}_c = speed-at-capacity (m/s)
 τ_m = perception reaction time calculated from macroscopic measures (s)

When simulating the Gipps model for this study additional constraints were added to the calculations; the simulated velocity was held at a minimum of 0.1 m/s.

Intelligent Driver Model (IDM)

The Intelligent Driver Model (IDM) was developed as a high-fidelity model trying to reproduce traffic as realistically as possible, with a small number of parameters, and realistic breaking reactions [16]. The authors of the IDM, as shown in Equation (5), cite the Gipps model as achieving these goals, though they attempt to overcome its limitations by introducing instabilities or hysteresis effects for vanishing fluctuations.

$$\ddot{x}_{n+1}(t) = \ddot{x}_{d-max} \left\{ 1 - \left[\frac{\dot{x}_{n+1}(t)}{\dot{x}_d} \right]^\delta - \left[\frac{(\Delta x_j - l_n) + (\dot{x}_{n+1}(t) \cdot \tau_S) + \frac{\dot{x}_{n+1}(t) |\Delta \dot{x}_{n \rightarrow n+1}(t)|}{2 \cdot \sqrt{\ddot{x}_{d-max} |\ddot{x}_{d-min}|}}}{\Delta x_{n \rightarrow n+1}(t) - l_n} \right]^2 \right\} \quad (5)$$

Where: δ = acceleration exponent
 τ_S = safe time headway
 l_n = approximate length of vehicle n, taken to be 4.5 meters

The IDM examines the maximum possible acceleration, and combines both acceleration and deceleration strategies into the formulation. The acceleration strategy takes the instantaneous ratio of the current velocity and desired velocity, and raises this value by the acceleration exponent, taken to be a default value of 4 in the original documentation. The deceleration strategy examines the desired spacing as a function of velocity of the following vehicle and the difference in velocity between the leading and following vehicles, and squares the result of this desired spacing divided by the current space headway. Effectively, this formulation balances the pull of the desired velocity against the push of the desired spacing.

When simulating the Intelligent Driver model for this study additional constraints were added to the calculations; the simulated velocity was held at a minimum of 0.1 m/s.

Rakha-Pasumathy-Adjerid (RPA) Model

Similar to the Gipps model, the RPA model seeks to use parameters that correspond to characteristics of drivers and vehicles, enabling the calibration parameters to be assessed based on objective measures [17–19]. The model uses the Van Aerde steady-state traffic stream model first proposed in a nonlinear, single-regime functional form in 1995, as seen in Equation (6).

$$\Delta x_{n \rightarrow n+1}(t) = c_1 + \frac{c_2}{\dot{x}_d - \dot{x}_{n+1}(t)} + c_3 \cdot \dot{x}_{n+1}(t) \quad (6)$$

This formulation provides the space headway of the leader-follower pair at time (t) using the velocity of the follower vehicle and four driver/vehicle calibrated parameters. The first calibration parameter, c_1 , is the fixed distance headway constant (m). The second calibration parameter, c_2 , is the first variable headway constant (m^2/s), and provides a measure of the driver's desire to return to their desired speed. The third calibration parameter, c_3 , is the second variable headway constant (s), analogous to the driver sensitivity parameter in the Pipes model. It has been shown that constraints may be applied on the three calibration parameters by considering limitations experienced at jam conditions and capacity conditions, subscripts j and c respectively, as in Equation (7) [20], [21].

$$c_1 = \frac{\Delta x_j \cdot \dot{x}_f}{\dot{x}_c^2} (2\dot{x}_c - \dot{x}_f); \quad c_2 = \frac{\Delta x_j \cdot \dot{x}_f}{\dot{x}_c^2} (\dot{x}_f - \dot{x}_c)^2; \quad c_3 = \left(\frac{\Delta x_c}{\dot{x}_c} - \frac{\Delta x_j \cdot \dot{x}_f}{\dot{x}_c^2} \right) \quad (7)$$

The application of these constraint conditions and the translation of the Van Aerde model into a speed formulation results in the Equation (8).

$$\dot{x}_{n+1}(t) = \frac{-c_1 + c_3 \cdot \dot{x}_d + \Delta x_{n \rightarrow n+1}(t) - \sqrt{[c_1 - c_3 \cdot \dot{x}_d - \Delta x_{n \rightarrow n+1}(t)]^2 - 4 \cdot c_3 [\Delta x_{n \rightarrow n+1}(t) \cdot \dot{x}_d - c_1 \cdot \dot{x}_d - c_2]}}{2 \cdot c_3} \quad (8)$$

The RPA model imposes limitations on the steady-state Van Aerde model to ensure collision avoidance, and to account for vehicle dynamics constraints, as demonstrated by Park et al [22]. The collision avoidance component is shown in Equation (9).

$$\dot{x}_{n+1}(t) = \sqrt{[\dot{x}_n(t)]^2 + 11.76 \cdot [\Delta x_{n \rightarrow n+1}(t) - \Delta x_j]} \quad (9)$$

A detailed explanation of the application of the vehicle dynamics model, as seen in Equation (10) is beyond the scope of this study, but can be found in a publication by Rakha *et al.* [23].

$$\dot{x}_{n+1}(t) = \dot{x}_{n+1}(t - \Delta t) + \Delta t \cdot \frac{F_{n+1}(t - \Delta t) - R_{n+1}(t - \Delta t)}{\text{mass}_{n+1}} \quad (10)$$

$$\text{Where: } F_{n+1}(t - \Delta t) = \min \left[3,600 * \eta * \frac{\gamma * P}{\dot{x}_{n+1}(t - \Delta t)}, 9.8066 * M_{ta} * \mu \right]$$

$$R_{n+1}(t - \Delta t) = 0.047285 * C_d * A_f * \dot{x}_{n+1}(t - \Delta t)^2 + 9.8066 * \text{mass}_{n+1} * C_r [c_{r2} * \dot{x}_{n+1}(t - \Delta t) + c_{r3}]$$

The formulation included herein is nearly identical to that of the formulation provided in Rakha *et al.* [21], with the exception of gamma (γ) being applied to engine power, where gamma is equal to the maximum throttle input observed for a given driver in the dataset.

The parameters included in the vehicle dynamics model not previously defined include:

$$\begin{aligned} F_{n+1} &= \text{resultant force (N)} \\ R_{n+1} &= \text{total resistive force (N)} \\ \text{mass}_{n+1} &= \text{vehicle mass (kg) of vehicle } n + 1 \end{aligned}$$

η	=	<i>driveline efficiency (unitless), taken as 0.7 herein</i>
γ	=	<i>acceleration reduction factor (unitless), taken from the maximum measured percentage throttle depression for each driver herein</i>
P	=	<i>vehicle power (kW)</i>
M_{ta}	=	<i>mass of the vehicle on the tractive axle (kg), taken to be 55% of total vehicle mass herein</i>
μ	=	<i>coefficient of roadway adhesion (unitless), taken as 0.6 herein</i>
C_d	=	<i>drag coefficient (unitless)</i>
A_f	=	<i>vehicle frontal area (meters squared)</i>
C_r	=	<i>rolling coefficient (unitless), taken as 0.00125 herein</i>
c_{r2}, c_{r3}	=	<i>rolling resistance coefficients (unitless), taken as 0.0328 and 4.575 herein, respectively</i>

Recent research, to be published elsewhere, demonstrates the need for a fourth component added to the RPA model to account for driver preferences when forced to decelerate [24]. It is found that when a vehicle encounters a space headway shorter than is desired, such as on a multilane highway when a leading vehicle first enters the driver's lane from an adjacent lane, the driver will decelerate by coasting so long as safety considerations are met. The rate of deceleration when coasting is found to be approximately equal to the deceleration predicted by the vehicle dynamics model, seen in Equation (10) when the value of the throttle, γ , is set to zero.

The components of the RPA model, being represented by Equations (8), (9), and (10) are implemented as shown in Equation (11). A full explanation can be found elsewhere [24].

$$\dot{x}_{n+1}(t) = \max[\min(\text{Eq. 9}, \text{Eq. 10 with } \gamma = 0), \min(\text{Eq. 8}, \text{Eq. 9}, \text{Eq. 10})] \quad (11)$$

PARAMETER CALIBRATION

Each car-following model predicts the time-space trajectory of a following vehicle when provided with the time-space trajectory of a leading vehicle, and the original location and velocity of the following vehicle. The parameters of each model are calibrated such that the resulting simulated behavior matches the observed behavior as closely as possible. To compute these calibrated parameter values it is necessary to generate observed and simulated vehicle trajectories, set limiting bounds on the parameter values, define an error function, and select an optimization method to minimize the error objective function.

Discrete Time Generation of Vehicle Trajectories

In the case of the GHR, and Gipps models, the predicted acceleration of the following vehicle at time-step (t) is dependent on the vehicle trajectory information at time-step ($t - \tau$), therefore all location (x), velocity (\dot{x}), and acceleration (\ddot{x}) information for the simulated vehicle trajectory that occurs during the initial time τ is set equal to the observed information during that time.

The GHR, and IDM methodologies each generate the anticipated acceleration of the following vehicle in a given time-step: $\ddot{x}_{n+1}(t)$. This information in itself does not provide the vehicle trajectory of the following vehicle, which must be estimated from the predicted

acceleration. The forward Euler method was used to solve for the vehicle position and speed, as shown in Equations (12) and (13).

$$\dot{x}_{n+1}(t) = \dot{x}_{n+1}(t - \Delta t) + \Delta t \cdot \ddot{x}_{n+1}(t - \Delta t) \quad (12)$$

$$x_{n+1}(t) = x_{n+1}(t - \Delta t) + \Delta t \cdot \dot{x}_{n+1}(t - \Delta t) \quad (13)$$

Alternatively, the Gipps and RPA models generate a predicted velocity value for a given time-step, with a translation to acceleration as shown in Equation (14).

$$\ddot{x}_{n+1}(t) = \Delta t^{-1} \cdot [\dot{x}_{n+1}(t + \Delta t) - \dot{x}_{n+1}(t)] \quad (14)$$

Parameter Feasible Ranges

When performing model calibration it is necessary to set upper and lower limits for the values of each parameter. Many of the parameters can be fixed outright for each driver by examining both the raw dataset and by examining the macroscopic data. The macroscopic data is analyzed using a heuristic automated tool (SPD-CAL), described in a publication by Rakha and Arafeh [25]. The desired velocity for each driver is taken from the values generated by SPD-CAL, and is used in the Gipps, IDM, and RPA models.

The minimum and maximum acceptable acceleration values for the follower vehicle are a result of taking the minimum and the maximum observed values from each driver. The anticipated maximum deceleration rate of the leading vehicle is determined from Gipps' assumptions, as previously shown in Equation (2). A mathematical analysis of the Gipps model by Wilson [13], and subsequently by Rakha and Wang [14] show that linear continuity may be lost when $\ddot{x}_{d-min} < \ddot{x}_{d-min,n}$, whereas the original formulation by Gipps [12] has $\ddot{x}_{d-min} < \ddot{x}_{d-min,n}$ only when $\ddot{x}_{d-min} < 3$, and $\ddot{x}_{d-min,n} = \frac{3+\ddot{x}_{d-min}}{2}$ otherwise. The original Gipps formulation of $\ddot{x}_{d-min,n}$ is held herein, but further study is warranted on the calculation of this parameter.

The various parameter bounds optimized using microscopic simulation are based on recommendations in the literature [11], [16]. Calibration is conducted using the evolutionary non-linear approach applied in Microsoft Excel version 14.0, which utilizes a genetic algorithm to find local minima and a multi-start function to find global minima. It was necessary to use a heuristic calibration methodology due to the large quantity of data being analyzed and the nonlinear nature of the objective function.

Optimization Functions to Match Simulated and Observed Results

The calibration of car-following models consists of determining values for the variable parameters that result in the best match between the observed behavior of a following vehicle and the simulated behavior of the same following vehicle, using the observed behavior of a leading vehicle as model input. Punzo and Simonelli [26] examine a variety of calibration methods, citing that the error tests in common use are the root mean square error (RMSE), the root mean square percentage error (RMSPE), and Theil's inequality coefficient (U). It is noted that the choice of performance measure in the objective function may condition the results. Because it is desirable to compare the error measures both between models and between individual drivers for a given model, the authors herein have decided to use a variant of the

RMPSE, taking both speed and space headway as objective measures, as shown in Equation (15).

$$F(\dot{x}_{n+1,sim}(t), \Delta x_{n \rightarrow n+1,sim}(t)) = \sqrt{\frac{\sum(\dot{x}_{n+1,obs}(t) - \dot{x}_{n+1,sim}(t))^2}{\sum(\dot{x}_{n+1,obs}(t))^2}} + \sqrt{\frac{\sum(\Delta x_{n \rightarrow n+1,obs}(t) - \Delta x_{n \rightarrow n+1,sim}(t))^2}{\sum(\Delta x_{n \rightarrow n+1,obs}(t))^2}} \quad (15)$$

RESULTS OF PARAMETER CALIBRATION

A listing of the calibrated parameters for the eight drivers, as well as aggregate results, is given in TABLE 2 along with corresponding measures of error.

TABLE 2 (a) Results for the Gaxis-Herman-Rothery model

Parameter	Min	Max	D124	D304	D316	D350	D358	D363	D367	D462	Agg.
τ_{GHR}^a	1.0	3.0	2.0	2.3	1.8	2.2	2.0	2.3	1.0	1.6	2.3
α^a	10	60	60.0	60.0	60.0	60.0	30.0	60.0	18.9	60.0	60.0
z_a^a	-0.5	1.0	0.28	-0.50	0.52	0.27	0.77	-0.42	0.26	0.39	0.29
l_a^a	1.5	2.5	2.10	1.59	2.09	2.06	2.01	1.50	1.60	2.41	2.07
z_d^a	0.0	1.0	0.00	0.92	0.00	0.00	0.00	0.29	0.00	0.00	0.00
l_d^a	1.5	3.0	1.95	3.00	1.82	1.84	1.51	2.44	1.52	2.24	1.94
No. Obs.	-	-	44,051	38,431	108,567	33,976	102,521	99,545	121,667	13,565	551,406
RMSPE	-	-	0.00079	0.00082	0.00096	0.00080	0.00104	0.00046	0.00104	0.00069	0.00033

a denotes values optimized through optimization

TABLE 2 (b) Results for the Gipps model

Parameter	D124	D304	D316	D350	D358	D363	D367	D462	Agg.
τ_m^b	0.8	0.4	1.3	1.2	1.4	0.8	1.3	0.4	1.1
Δx_{jam}^b	6.70	6.51	8.09	7.27	6.21	6.67	5.90	7.62	5.92
\dot{x}_d^b	29.14	31.94	26.81	26.06	32.22	31.94	26.22	31.94	28.31
\ddot{x}_{d-max}^c	4.167	2.778	2.778	3.472	4.167	3.472	5.948	1.852	5.948
\ddot{x}_{d-min}^c	-4.630	-2.778	-3.472	-5.556	-5.556	-4.861	-5.961	-2.451	-5.961
$\ddot{x}_{(n)-min}^c$	-3.815	-3.000	-3.236	-4.278	-4.278	-3.931	-4.481	-3.000	-4.481
No. Obs.	46,307	41,357	110,227	36,666	105,179	103,655	120,146	14,429	578,274
RMSPE	0.00064	0.00033	0.00030	0.00094	0.00028	0.00019	0.00040	0.00055	0.00014

b denotes values optimized using SPD-CAL

c denotes values observed from dataset

TABLE 2 (c) Results for the Intelligent Driver model

Parameter	Min	Max	D124	D304	D316	D350	D358	D363	D367	D462	Agg.
τ_S^a	1.0	3.0	1.32	3.00	2.52	2.09	2.37	2.37	1.90	2.20	1.72
Δx_{jam}^b	-	-	6.70	6.51	8.09	7.27	6.21	6.67	5.90	7.62	5.92
\dot{x}_d^b	-	-	29.14	31.94	26.81	26.06	32.22	31.94	26.22	31.94	28.31
\ddot{x}_{d-max}^c	-	-	4.167	2.778	2.778	3.472	4.167	3.472	5.948	1.852	5.948
\ddot{x}_{d-min}^c	-	-	-4.630	-2.778	-3.472	-5.556	-5.556	-4.861	-5.961	-2.451	-5.961
δ^a	10	40	12.40	10.00	28.86	17.96	16.74	12.26	17.44	10.00	16.79
No. Obs.	-	-	45,367	37,507	106,243	34,514	101,192	99,545	117,104	13,133	564,840
RMSPE	-	-	0.00142	0.00172	0.00101	0.00181	0.00069	0.00068	0.00057	0.00328	0.00026

a denotes values optimized through optimization

b denotes values optimized using SPD-CAL

c denotes values observed from dataset

TABLE 2 (d) Results for the Rakha-Pasumarthy-Adjerid model

Parameter	D124	D304	D316	D350	D358	D363	D367	D462	Agg.	
γ^c	0.631	0.600	0.710	0.537	0.576	0.529	0.764	0.639	0.764	
\ddot{x}_{d-min}^c	-4.630	-2.778	-3.472	-5.556	-5.556	-4.861	-5.961	-2.451	-5.961	
k_j^b	0.149	0.154	0.124	0.138	0.161	0.150	0.170	0.131	0.169	
q_c^b	0.948	1.000	0.523	0.611	0.514	0.975	0.569	1.000	0.662	
\dot{x}_c^b	23.56	16.67	26.81	22.31	19.14	19.06	17.89	22.22	28.31	
\dot{x}_d^b	29.14	31.94	26.81	26.06	32.22	31.94	26.22	31.94	28.31	
Vehicle	P^c	90	90	90	90	145	145	90 ^d	119	varies
	$mass^c$	1190	1090	1090	1090	1375	1375	1090 ^d	1900	varies
	C_d^c	0.36	0.40	0.40	0.40	0.40	0.40	0.40 ^d	0.50	varies
	A_f^c	2.06	2.00	2.00	2.00	2.18	2.18	2.00 ^d	2.94	varies
No. Obs.	47,623	41,819	114,211	39,625	110,938	105,573	126,170	14,645	600,604	
RMSPE	0.00063	0.00031	0.00026	0.00082	0.00026	0.00015	0.00038	0.00035	0.00012	

b denotes values optimized using SPD-CAL

c denotes values observed from the dataset

d denotes assumed values due to a lack of documented information

TABLE 2(e) Summary table comparing error results

Parameter	D124	D304	D316	D350	D358	D363	D367	D462	Aggregate
<i>GHR</i>	0.00079	0.00082	0.00096	0.00080	0.00104	0.00046	0.00104	0.00069	0.00033
<i>Gipps</i>	0.00064	0.00033	0.00030	0.00094	0.00028	0.00019	0.00040	0.00055	0.00014
<i>IDM</i>	0.00142	0.00172	0.00101	0.00181	0.00069	0.00068	0.00057	0.00328	0.00026
<i>RPA</i>	0.00063	0.00031	0.00026	0.00082	0.00026	0.00015	0.00038	0.00035	0.00012

The RPA model is found to provide the best overall fit to the naturalistic dataset analyzed herein, with the Gipps model ranked second. As formulated herein, the GHR, Gipps, and IDM models each have six calibration parameters, and can be considered to be of equivalent complexity. The RPA model has six calibration parameters other than those related to the vehicle dynamics component, with the specific vehicle driven serving as a seventh parameter, determining all of the elements of the vehicle dynamics model analyzed herein. Though there is an increase in complexity from the Gipps model to the RPA model, there is also a corresponding decrease seen in the error function. Because the naturalistic data inherently includes information regarding the specific vehicle dynamics of each driver, the quantitative results suggest that the RPA model is most appropriate to fully utilize this type of dataset.

Due to the close proximity of the error values determined for the RPA model and the Gipps model, additional statistical analysis was conducted to determine significance. By using the parameters calculated for individual drivers, the data was re-processed to generate error values from the objective function for each individual car-following event. The distribution of these events was found to be non-normal, requiring non-parametric analysis. By pairing the results of the various models using the individual events, a Wilcoxon Signed-Rank Test was performed using the JMP Pro statistical analysis software. With a sample size of 2,238 individual events, the probability that the RPA model will perform better than the Gipps model was determined to be 0.9977. All other relationships between the four models were found to be statistically significant as well, with probabilities greater than or equal to 0.9999.

Driver 316 is selected for further analysis for two reasons; the dataset includes a large amount of data for this driver, and the relative goodness of fit for each of the models is approximately equal between this particular driver and the aggregate data results. To examine qualitative data, **FIGURE 5** displays a sample interaction diagram, in the form of speed vs. spacing for each of the four car-following models analyzed herein. The charts display observed data points in black, with simulated data points in grey. In the case of the Gipps and RPA models, there exists a steady-state interpretation of each model, displayed as white lines.

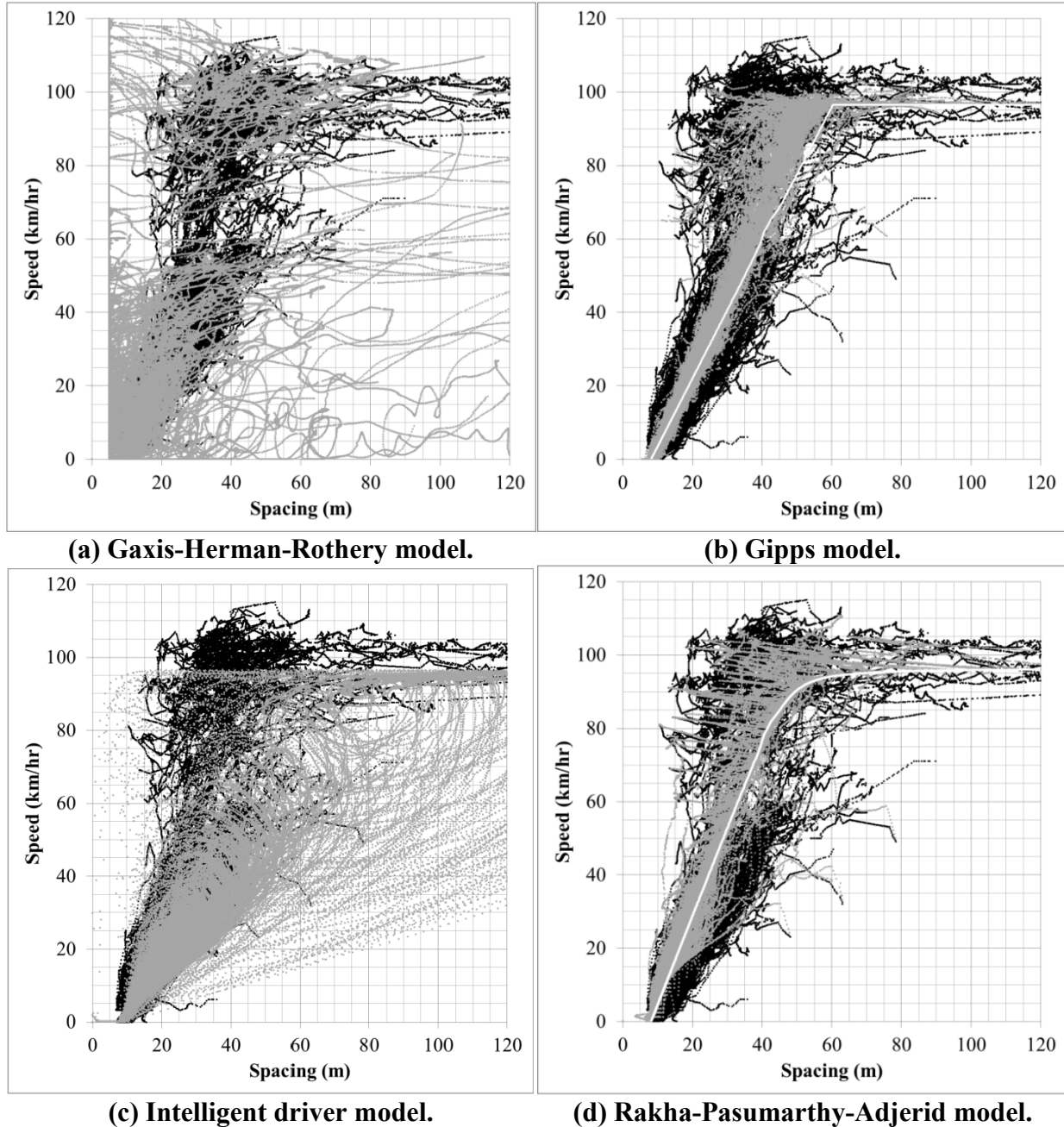
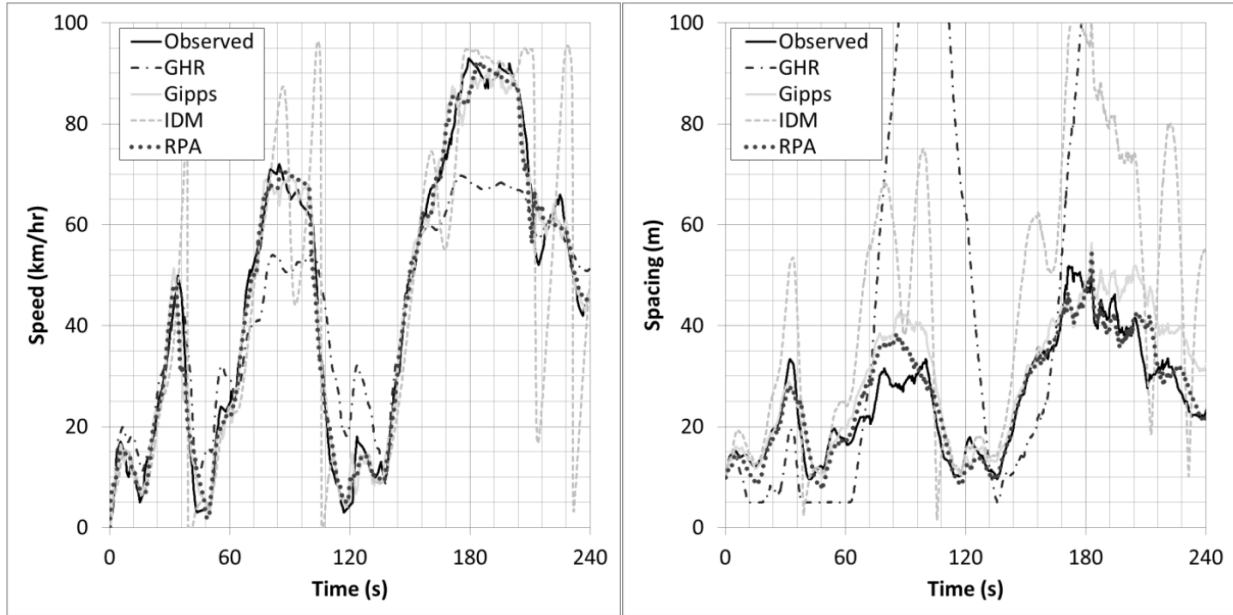


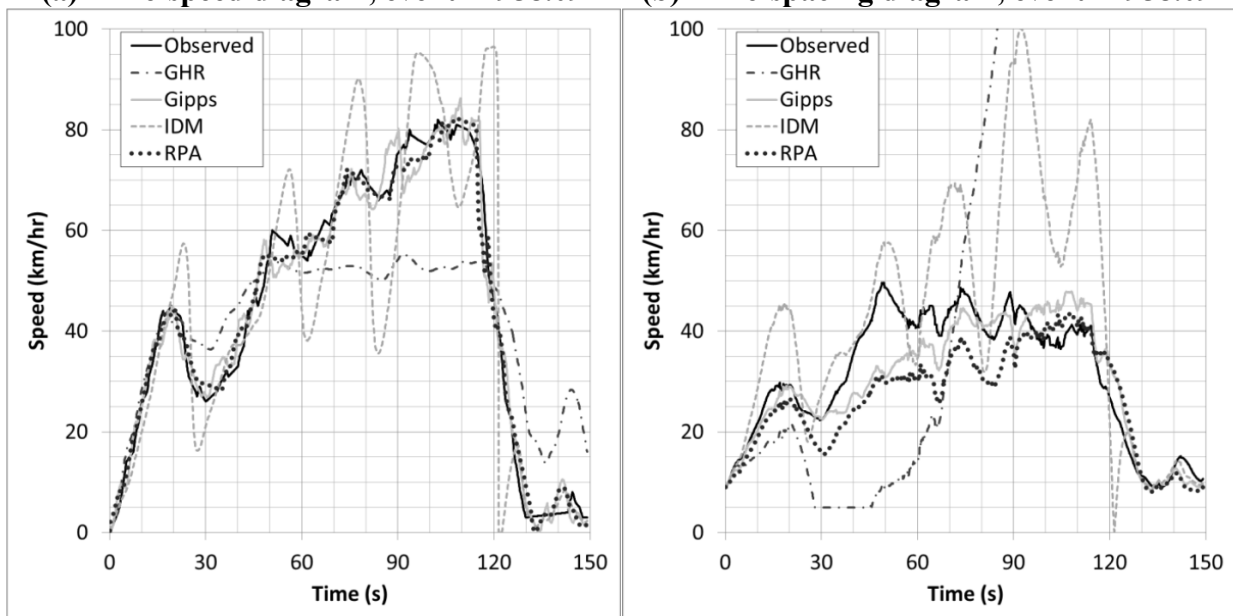
FIGURE 5 Driver 316 interaction diagram showing spacing vs. speed for the (a) GHR, (b) Gipps, (c) IDM, and (d) RPA models.

As a qualitative measure it is seen that the GHR and Intelligent Driver models are not able to replicate the car-following behavior in the naturalistic dataset, with simulated speed vs. spacing relationships significantly different from the breadth of the observed behavior. On the other hand, the Gipps and RPA models both appear to produce variability that is less than that observed in the field data. The RPA model appears to capture the steady-state of deceleration behavior considerably well (congested data to the left of the steady-state model). To further examine the qualitative information, **FIGURE 6** displays sample trajectory data.



(a) Time-speed diagram, event 21958.09

(b) Time-spacing diagram, event 21958.09



(c) Speed-time diagram, event 22626.08

(d) Spacing-time diagram, event 22626.08

FIGURE 6 Sample car-following events; event 21958.09 (a) time-speed diagram and (b) time-spacing diagram, and event 22626.08 (c) time-speed diagram and (d) time-spacing diagram.

Sampling two individual events from driver 316, it can be seen that the trajectory data for the various models analyzed herein qualitatively supports the observations made from the fundamental diagram view of the simulated results. The GHR and Intelligent Driver models have fluctuations in them that are far in excess of those from the observed driver, while the trajectories simulated by the Gipps and RPA models have fewer and smaller fluctuations than what is seen from the observed driver behavior. In general the RPA model mimics the observed driver behavior very well.

CONCLUSIONS AND RECOMMENDATIONS

The 100-Car Study database used herein includes 20,000,000 minutes worth of data, recorded at a frequency of 10 Hz (every 0.1 seconds), distributed across 108 drivers. Due to current limitations in computing power, it proved infeasible to perform analysis on the database in its entirety. A process was developed to identify car-following events along a stretch of highway traveled by multiple drivers. By examining the location data recorded by GPS in a GIS application, the Dulles Airport Access Road was observed to be a regular commuting route for 15 of the test drivers. Selecting only the data along this roadway generated by the drivers during their commute reduced the data to 30,000 minutes, and identifying incomplete data for various drivers further reduced the data to 16,000 minutes. Final data validation resulted in approximately 1,000 minutes of data, representing 2,200 individual car-following events experienced by eight drivers. If the percentage of valid data extracted in this study is indicative of the overall database, it follows that there is approximately 60,000 minutes of valid car-following behavior stored in the 100-Car Study database which has yet to be processed and analyzed.

Post processing of naturalistic data is an important phase in the data reduction process. The radar equipment used for the 100-Car Study tracked seven objects simultaneously; however, because of significant errors in the object tracking, all car-following events had to be manually verified using recorded video data. The presence of both onboard diagnostic and GPS speed data provided an opportunity to independently validate the two data sources. The analysis demonstrated that significant errors were observed in both sources of speed measurements, resulting in a significant loss in useable data. Identifying speed measurement errors was simplified by computing the acceleration at each time-step and ensuring they were within the physical limitations of the vehicle. The examination of acceleration also demonstrated that the onboard diagnostic values were updated less frequently than the values were reported, requiring interpolation of the data.

Of the four car-following models calibrated against the data, the Rakha-Pasumarthy-Adjerid (RPA) model performed best, followed by the Gipps model. Both the RPA and Gipps models performed significantly better than either the Gaxis-Herman-Rothery (GHR) model or the Intelligent Driver model (IDM). Based on fundamental diagram data the RPA and Gipps models display less variability in behavior in comparison to the observed data, but provide a significantly better match to the data when compared to the GHR or IDM models. In examining the qualitative results of the vehicle trajectory data, looking at the variation in speed and spacing over time, the paths simulated by the GHR and IDM models are seen to fluctuate significantly compared to the observed behavior, possibly an indication of an over-sensitive simulated driver; the RPA and Gipps models appear to maintain a close relationship with the observed behavior, with perhaps less variability in behavior than that of the observed driver.

The authors herein recommend that future analysis with naturalistic driving data be performed using the RPA model, due to its unique ability to incorporate the specific vehicle dynamics information that are available in the dataset. Though the processing of data from a naturalistic driving study can be costly, the unique combination of specific driver information, coupled with vast amounts of recorded data, can potentially shed light on a number of current topics of research in car-following behavior. The psychological underpinnings of driver behavior, questions of driver heterogeneity, the effects of hysteresis in traffic flow, and the relationship between roadway types and driver behavior are all areas of further research using this data.

ACKNOWLEDGEMENT

The authors acknowledge the financial support provided by the FHWA and the Mid-Atlantic University Transportation Center (MAUTC) in conducting this research effort.

REFERENCES

- [1] T. Kim, D. Lovell, and Y. Park, "Limitations of Previous Models on Car-Following Behavior and Research Needs," in *Transportation Research Board, 82nd Annual Meeting of the*, 2003, no. 03.
- [2] S. Panwai and H. Dia, "Comparative Evaluation of Microscopic Car-Following Behavior," *IEEE Transactions on Intelligent Transportation Systems*, vol. 6, no. 3, pp. 314-325, Sep. 2005.
- [3] T. A. Dingus et al., "The 100-Car Naturalistic Driving Study Phase II – Results of the 100-Car Field Experiment," 2006.
- [4] R. E. Chandler, R. Herman, and E. W. Montroll, "Traffic Dynamics: Studies in Car Following," *Operations Research*, vol. 6, no. 2, pp. 165–184, Jan. 1958.
- [5] R. W. R. Rothery, R. Silver, R. Herman, and C. Torner, "Analysis of Experiments on Single-lane Bus Flow," *Operations Research*, vol. 12, no. 6, pp. 913-933, 1964.
- [6] A. D. May, *Traffic Flow Fundamentals*. Upper Saddle River, NJ: Prentice-Hall, Inc., 1990, pp. 1-464.
- [7] B. D. Greenshields, J. Bibbins, W. Channing, and H. Miller, "A Study of Traffic Capacity," in *Highway Research Board, Proceedings of the*, 1935, pp. 448-477.
- [8] A. Halati, H. Lieu, and S. Walker, "CORSIM - Corridor Traffic Simulation Model," in *Traffic Congestion and Traffic Safety in the 21st Century: Challenges, Innovations, and Opportunities*, 1997, pp. 570-576.
- [9] H. A. Rakha and B. Crowther, "Comparison and Calibration of FRESIM and INTEGRATION Steady-state Car-following Behavior," *Transportation Research Part A: Policy and Practice*, vol. 37, pp. 1-27, Jan. 2003.
- [10] L. A. Pipes, "An Operational Analysis of Traffic Dynamics," *Journal of Applied Physics*, vol. 24, no. 3, pp. 274–281, Jul. 1953.
- [11] M. Brackstone and M. McDonald, "Car-following: A Historical Review," *Transportation Research Part F: Traffic Psychology and Behaviour*, vol. 2, no. 4, pp. 181–196, Dec. 1999.
- [12] P. G. Gipps, "A Behavioural Car-following Model for Computer Simulation," *Transportation Research Part B: Methodological*, vol. 15, no. 2, pp. 105-111, Apr. 1981.
- [13] R. E. Wilson, "An analysis of Gipps's car-following model of highway traffic," *IMA journal of applied mathematics*, vol. 66, no. 5, pp. 509–537, 2001.
- [14] H. A. Rakha and W. Wang, "Procedure for Calibrating Gipps Car-Following Model," *Transportation Research Record: Journal of the Transportation Research Board*, vol. 2124, no. – 1, pp. 113-124, Dec. 2009.
- [15] H. A. Rakha, C. C. Pecker, and H. B. B. Cybis, "Calibration Procedure for Gipps Car-Following Model," *Transportation Research Record: Journal of the Transportation Research Board*, vol. 1999, pp. 115-127, Jan. 2007.
- [16] M. Treiber, A. Hennecke, and D. Helbing, "Congested Traffic States in Empirical Observations and Microscopic Simulations," *Physical Review E*, vol. 62, no. 2 Pt A, pp. 1805-24, Aug. 2000.
- [17] H. A. Rakha, "Validation of Van Aerde's Simplified Steady-state Car-following and Traffic Stream Model," *Transportation Letters: The International Journal of Transportation Research*, vol. 1, no. 3, pp. 227–244, 2009.

- [18] M. Van Aerde and H. A. Rakha, "Multivariate Calibration of Single Regime Speed-Flow-Density Relationships," *Vehicle Navigation and Information Systems, Proceedings of the 6th International Conference on*, pp. 334-341, 1995.
- [19] M. Van Aerde, "Single Regime Speed-Flow-Density Relationship for Congested and Uncongested Highways," *Transportation Research Board, 74th Annual Meeting of the*, 1995.
- [20] S. Demarchi, "A New Formulation for Van Aerde's Speed-flow-density Relationship (in Portuguese)," in *Pequisa e Ensino em Transportes, XVI Congresso De*, 2002.
- [21] H. A. Rakha, P. Pasumarthy, and S. Adjerid, "A simplified behavioral vehicle longitudinal motion model," *Transportation Letters: The International Journal of Transportation Research*, vol. 1, no. 2, pp. 95-110, 2009.
- [22] S. Park, H. A. Rakha, R. Alfelor, C. Y. D. Yang, and D. Krechmer, "Empirical Study of Impact of Icy Roadway Surface Condition on Driver Car-Following Behavior," in *Transportation Research Board, 90th Annual Meeting of the*, 2011, vol. 982, no. 617.
- [23] H. A. Rakha, M. Snare, and F. Dion, "Vehicle Dynamics Model for Estimating Maximum Light-Duty Vehicle Acceleration Levels," *Transportation Research Record: Journal of the Transportation Research Board*, vol. 1883, pp. 40-49, Jan. 2004.
- [24] J. D. Sangster and H. A. Rakha, "Application of Coasting Behavior to the Rakha-Pasumarthy-Adjerid (RPA) Car-Following Model." 2012.
- [25] H. A. Rakha and M. Azafeh, "Calibrating Steady-State Traffic Stream and Car-Following Models Using Loop Detector Data," *Transportation Science*, vol. 44, no. 2, pp. 151-168, Dec. 2010.
- [26] V. Punzo and F. Simonelli, "Analysis and comparison of microscopic traffic flow models with real traffic microscopic data," *Transportation Research Record: Journal of the Transportation Research Board*, vol. 1934, no. 1, pp. 53-63, Jan. 2005.

Enhancing and Calibrating the Rakha-Pasumarthy-Adjerid Car-Following Model using Naturalistic Driving Data

John Sangster, MS, PE

Center for Sustainable Mobility, Virginia Tech Transportation Institute
3500 Transportation Research Plaza
Blacksburg, VA 24061
Phone: (540) 231-1500
Email: johns80@vt.edu

Hesham Rakha, Ph.D., P.Eng. (corresponding author)

Charles E. Via, Jr. Department of Civil and Environmental Engineering
Center for Sustainable Mobility, Virginia Tech Transportation Institute
3500 Transportation Research Plaza
Blacksburg, VA 24061
Phone: (540) 231-1505
Fax: (540) 231-1555
Email: hrakha@vt.edu

ABSTRACT

The research presented in this paper analyzes the simplified behavioral vehicle longitudinal motion model, currently implemented in the INTEGRATION software, known as the Rakha-Pasumarthy-Adjerid (RPA) model. This model utilizes a steady-state formulation along with two constraints, namely: acceleration and collision avoidance. An analysis of the model using the naturalistic driving data identified a deficiency in the model formulation, in that it predicts more conservative driving behavior compared to naturalistic driving. Much of the error in simulated car-following behavior occurs when a car-following event is initiated. As a vehicle enters the lane in front of a subject vehicle, the spacing between the two vehicles is often much shorter than is desired; the observed behavior is that, rather than the following vehicle decelerating aggressively, the following vehicle coasts until the desired headway/spacing is achieved. Consequently, the model is enhanced to reflect this empirically observed behavior. Finally, a quantitative and qualitative evaluation of the original and proposed model formulations demonstrates that the proposed modification significantly decreases the modeling error and produces car-following behavior that is consistent with empirically observed driver behavior.

INTRODUCTION

There are many explanations of the importance of car-following models in microscopic traffic-simulation in the literature, with an informative and succinct example being that of Panwai and Dia from 2005 [1], who explain that traffic-simulation tools provide the ability to evaluate and control different scenarios in an environment that does not disrupt real-world traffic conditions.

Each car-following model predicts the time-space trajectory of a following vehicle when provided the time-space trajectory of a leading vehicle, along with the original location and velocity of the following vehicle. The parameters of each model are calibrated such that the resulting simulated behavior matches the observed behavior as closely as possible. To calibrate these parameters it is necessary to define limiting bounds for the parameter values, define an

error function, select an optimization methodology to minimize the objective function, and compare simulated to observed vehicle trajectories.

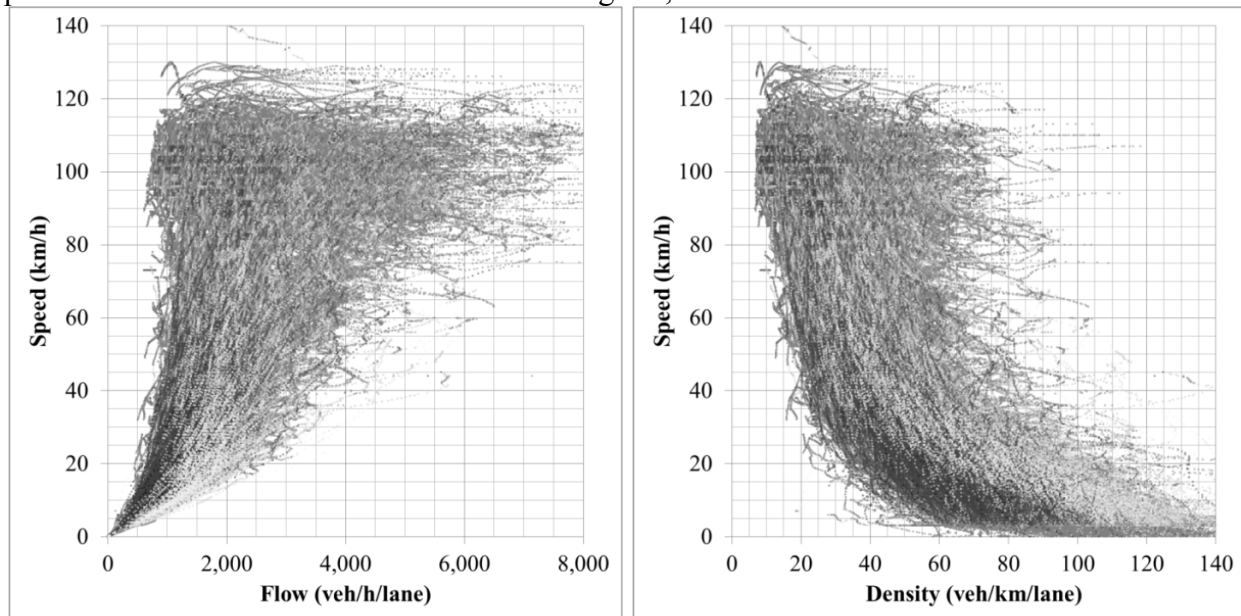
The data used to validate car-following models in the past has primarily come from test tracks, simulators, or loop detectors. These studies either have driver-specific information and bias from lack of real-world driving situations, or accurate real-world driving data from anonymous drivers. Only recently has naturalistic driving data become available as an analysis data source [2].

The large size of the database generated by a naturalistic driving study requires data reduction to be conducted using a carefully planned procedure. In the case of the Hundred Car Study, the initial dataset includes 108 individual drivers, with nearly 337,000 hours of data collected across 207,000 trips, which results in more than 12 billion database observations using a sampling frequency of 0.1 seconds. The data analyzed herein is identified using a geographic information system (GIS) application to visually select specific routes and drivers, exporting pertinent data to define trips of interest. Data validation is conducted on the selected data by examining outlier information. Some post-processing is necessary in cases where information is updated less often than is sampled.

Naturalistic data is particularly useful for car-following models which employ vehicle dynamics constraints, such as the Rakha-Pasumarty-Adjerid (RPA) model, examined herein. The vehicle dynamics constraints are based directly on the characteristics of the vehicle, which are included as part of a naturalistic database.

DATASET

The data used herein represents a subset of the total naturalistic driving database generated by the Hundred Car Study project conducted by the Virginia Tech Transportation Institute. The complete database includes 108 individual drivers, with 337,000 hours of data collected during 207,000 trips. The car-following event data used herein was recorded along a 14 km section of the Dulles Airport Access Road, in order to maintain facility homogeneity. Visualization is presented with the fundamental interaction diagram, as shown in FIGURE 1.



(a) Flow vs. speed

(b) Density vs. speed

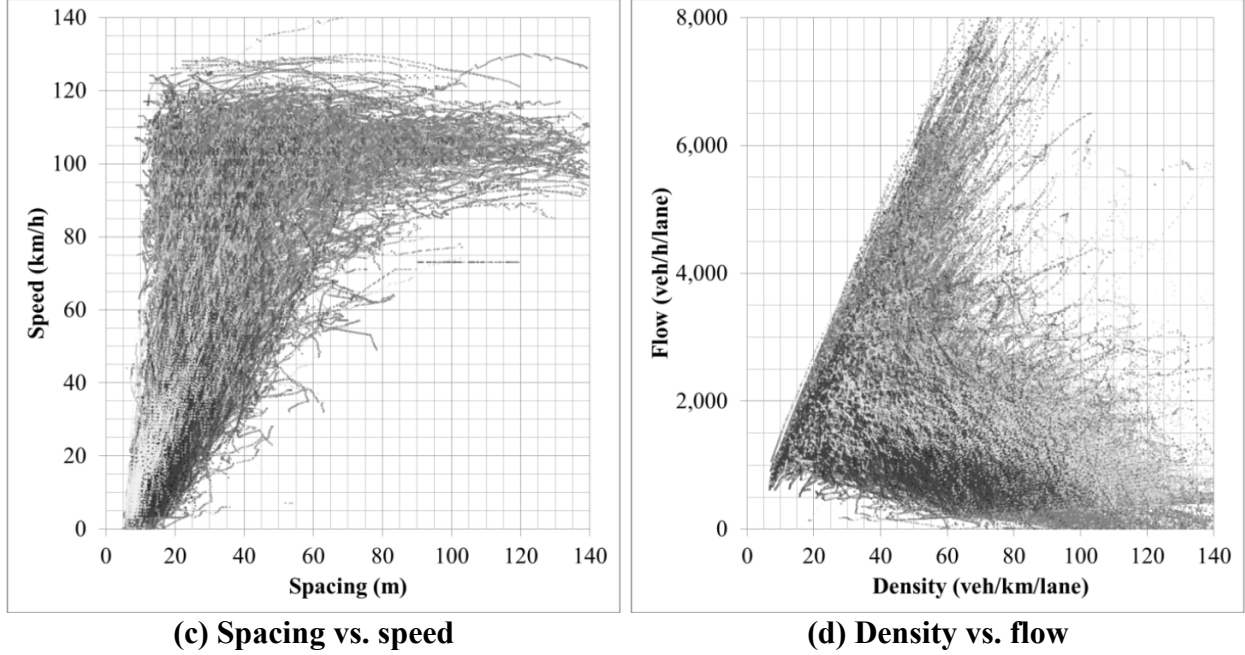


FIGURE 1 Combined fundamental diagram for car-following event data; displaying (a) flow vs. speed, (b) density vs. speed, (c) spacing vs. speed, and (d) density vs. flow.

The dataset used includes 1,732 car-following events, totaling 789 minutes, representing eight individual drivers. The data from the eight drivers is aggregated into four views of the fundamental diagram, with grayscale used to indicate steady-state conditions separately from acceleration and deceleration regimes. The darkness of the data points indicates the magnitude of acceleration, with near-black points indicating high acceleration levels, near-white points indicating high deceleration levels, and grey points indicating steady-state travel.

THE RAKHA-PASUMARTHY-ADJERID CAR-FOLLOWING MODEL

The Rakha-Pasumarthi-Adjerid (RPA) model is a simplified behavioral vehicle longitudinal motion model, currently incorporated in the INTEGRATION traffic simulation software. This model is comprised of three components, which respectively define steady-state traffic stream behavior, provide a collision avoidance component, and limit the simulated acceleration based on vehicle dynamics. Taking the minimum value of the three components yields the simulated velocity for a given time-step. It should be noted that the addition of the vehicle dynamics constraint reverts the model from a first-order to a second-order traffic stream model and allows for the capture of important phenomenon including the capacity drop associated with departures from congested states.

First-order Steady-state Car-following Model

The RPA model uses the Van Aerde first-order steady-state model first proposed as a nonlinear, single-regime functional form by Van Aerde and Rakha in 1995, as seen in Equation (1) [3].

$$\Delta x_{n \rightarrow n+1}(t) = c_1 + \frac{c_2}{\dot{x}_d - \dot{x}_{n+1}(t)} + c_3 \cdot \dot{x}_{n+1}(t) \quad (1)$$

Where: $\Delta x_{n \rightarrow n+1}(t)$ = the distance between the front of the leading vehicle (n) and the front of the following vehicle ($n+1$) at time (t), in (m).

$c_1, c_2, c_3 =$ Parameters used for the Van Aerde steady-state model, in (m), (m^2/s), and (s), respectively.

$\dot{x}_d =$ velocity desired by driver of vehicle $n + 1$, in (m/s). This is also known as the free-flow speed in the literature.

$\dot{x}_{n+1} =$ velocity of vehicle $n + 1$, in (m/s).

This formulation provides the space headway of the leader-follower pair at time (t) using the velocity of the follower vehicle and four calibration parameters. The first calibration parameter, c_1 , is the fixed distance headway constant in (m), and is analogous to vehicle spacing at jam density. The second calibration parameter, c_2 , is the first variable headway constant in (m^2/s), and provides a measure of the driver's desire to return to his/her desired speed. The third calibration parameter, c_3 , is the second variable headway constant in (s), analogous to the driver sensitivity parameter in the Pipes model. It has been shown that using boundary conditions the microscopic parameters can be related to macroscopic parameters, as demonstrated in Equation (2) [4].

$$c_1 = \frac{\Delta x_j \cdot \dot{x}_d}{\dot{x}_c^2} (2\dot{x}_c - \dot{x}_d); \quad c_2 = \frac{\Delta x_j \cdot \dot{x}_d}{\dot{x}_c^2} (\dot{x}_d - \dot{x}_c)^2; \quad c_3 = \left(\frac{\Delta x_c}{\dot{x}_c} - \frac{\Delta x_j \cdot \dot{x}_d}{\dot{x}_c^2} \right) \quad (2)$$

Where: $\dot{x}_c =$ velocity at capacity also known as the critical velocity in the literature, in (m/s).

$\Delta x_c =$ vehicle spacing at capacity, in (m).

$\Delta x_j =$ vehicle spacing at jam density, in (m).

The application of these constraint conditions and the translation of the Van Aerde model into a speed formulation results in the Equation (3).

$$\dot{x}_{n+1}^{(1)}(t) = \frac{-c_1 + c_3 \cdot \dot{x}_d + \Delta x_{n \rightarrow n+1}(t) - \sqrt{[c_1 - c_3 \cdot \dot{x}_d - \Delta x_{n \rightarrow n+1}(t)]^2 - 4 \cdot c_3 [\Delta x_{n \rightarrow n+1}(t) \cdot \dot{x}_d - c_1 \cdot \dot{x}_d - c_2]}}{2 \cdot c_3} \quad (3)$$

In order to ensure that the speed estimates are realistic the square root term should be positive.

This is achieved if the model parameters satisfy $\Delta x_c \geq \Delta x_j \left(2 - \frac{\dot{x}_c}{\dot{x}_d} \right)$ [4].

Collision Avoidance Model

The RPA model imposes limitations on the steady-state Van Aerde model to ensure collisions do not occur under non-steady-state conditions (e.g. a vehicle is approaching a slower vehicle ahead of it) and to account for vehicle dynamics constraints, as demonstrated by Park et al. [5]. The collision avoidance component is shown in Equation (4).

$$\dot{x}_{n+1}^{(2)}(t) = \sqrt{[\dot{x}_n(t)]^2 + 2 \cdot [\Delta x_{n \rightarrow n+1}(t) - \Delta x_j]} \quad (4)$$

Equation (4) is based on a derivation of the maximum distance a vehicle can travel to decelerate from its initial speed to the speed of the leading vehicle without colliding with it, maintaining the minimum jam density spacing behind the lead vehicle when it comes to a complete stop. This condition only applies when the following vehicle is traveling at a speed higher than the speed of the lead vehicle. Within the INTEGRATION software, microscopic traffic simulation employs the collision avoidance limitation when the time headway between the

two vehicles is less than 50 seconds. The limited application of the constraint ensures that a following vehicle will not adjust its behavior based on leading vehicles that are beyond the influence zone.

Vehicle Dynamics Model

A point of contention with state-of-the-practice car-following models is that realistic vehicle accelerations are not always maintained. The resistive forces acting on a vehicle's forward motion include air resistance, grade resistance, and rolling resistance. A vehicle is able to accelerate based on the creation of engine tractive force that exceeds the combined effect of the resistance forces. A detailed explanation of the application of the vehicle dynamics model is beyond the scope of this study, and is found in an earlier publication by Rakha et al. [6]. The maximum feasible velocity at time (t) is an expression of the previous time-step's velocity and the maximum feasible acceleration produced by the vehicle, as seen in Equation (5).

$$\dot{x}_{n+1}^{(3)}(t) = \dot{x}_{n+1}(t - \Delta t) + \Delta t \cdot \frac{F_{n+1}(t-\Delta t) - R_{n+1}(t-\Delta t)}{mass_{n+1}} \quad (5)$$

$$\text{Where: } F_{n+1}(t - \Delta t) = \min \left[3,600 * \eta * \frac{\gamma * P}{\dot{x}_{n+1}(t-\Delta t)}, 9.8066 * M_{ta} * \mu \right]$$

Given that: F_{n+1} = resultant force (N)

η = driveline efficiency (unitless), taken as 0.7 herein

γ = vehicle throttle level ranging from 0.0 to 1.0 (unitless), taken from the maximum measured percentage throttle depression for each driver herein

P = vehicle power (kW)

M_{ta} = percentage mass of the vehicle on the tractive axle (unitless), taken to be 55% of total vehicle mass

μ = coefficient of roadway adhesion (unitless), taken as 0.6 herein

$$\text{And: } R_{n+1}(t - \Delta t) = 0.047285 * C_d * A_f * \dot{x}_{n+1}(t - \Delta t)^2 + 9.8066 * mass_{n+1} * C_r [c_{r2} * \dot{x}_{n+1}(t - \Delta t) + c_{r3}]$$

Given that: R_{n+1} = total resistive force (N)

C_d = drag coefficient (unitless), vehicle specific.

A_f = vehicle frontal area (m^2), vehicle specific.

$mass_{n+1}$ = vehicle mass (kg) of vehicle $n + 1$

C_r = rolling coefficient (unitless)

c_{r2}, c_{r3} = rolling resistance coefficients (unitless)

The formulation included herein is nearly identical to that of the formulation provided in Rakha et al. [6], with the exception of gamma (γ) being applied to engine power, where gamma is equal to the maximum throttle level observed to be used by a given driver.

PARAMETER CALIBRATION

Car-following models predict the trajectory of a subject following another lead vehicle when the trajectory of a lead vehicle and the original location and velocity of the following vehicle (also known as the initial conditions) are provided. The parameters of each model are calibrated such that the resulting simulated behavior matches the observed behavior as closely as possible. In

calibrating the model parameters it is necessary to generate observed and simulated vehicle trajectories, set limiting bounds for the parameter values, define an error function, and select an optimization method to minimize the error between the estimated and observed behavior.

Discrete Time Generation of Vehicle Trajectories

The RPA methodology generates the anticipated velocity of the following vehicle in a given time-step using the estimated acceleration, $\ddot{x}_{n+1}(t)$. The forward Euler method is used to estimate the velocity, by way of Equations (6) and (7).

$$x_{n+1}(t) = x_{n+1}(t - \Delta t) + \Delta t \cdot \dot{x}_{n+1}(t - \Delta t) \quad (6)$$

$$\ddot{x}_{n+1}(t) = \Delta t^{-1} \cdot [\dot{x}_{n+1}(t + \Delta t) - \dot{x}_{n+1}(t)] \quad (7)$$

Parameter Calibration

The calibration of the model parameters entailed two calibration efforts, namely: calibrating the steady-state and non-steady-state behavior. The calibration of the steady-state behavior was conducted using a heuristic automated tool (SPD-CAL), described in the literature [7]. This entailed calibrating the desired velocity for each driver.

The calibration of the non-steady-state behavior entailed calibrating the vehicle deceleration and acceleration parameters. Vehicle-specific parameters were extracted from automotive websites without the need for calibration. The maximum acceptable deceleration of the subject vehicle was extracted from the empirical data. Calibration of the remaining parameters was conducted using the evolutionary non-linear solver in Microsoft Excel version 14.0, which utilizes a genetic algorithm (GA) to find local minima and a multi-start function to find the global minimum. It was necessary to use a heuristic calibration methodology given that the feasible region and objective function were non-convex.

Optimization Function

The objective function used was a variant of the Root Mean Percent Squared Error (RMPS_e) considering both the vehicle speed and spacing, as demonstrated in Equation (8).

$$F(\dot{x}_{n+1,sim}(t), \Delta x_{n \rightarrow n+1,sim}(t)) = \sqrt{\frac{\sum(\dot{x}_{n+1,obs}(t) - \dot{x}_{n+1,sim}(t))^2}{\sum(\dot{x}_{n+1,obs}(t))^2}} + \sqrt{\frac{\sum(\Delta x_{n \rightarrow n+1,obs}(t) - \Delta x_{n \rightarrow n+1,sim}(t))^2}{\sum(\Delta x_{n \rightarrow n+1,obs}(t))^2}} \quad (8)$$

PARAMETER CALIBRATION RESULTS

Initially, a first-order traffic stream model was calibrated using the empirical data. Subsequently, a second-order model was calibration by adding the collision avoidance and acceleration constraints to the first-order model. It should be noted that a second-order model, unlike a first-order model, can capture the empirically observed reduction in discharge flow after the onset of congestion.

While all seven drivers from the naturalistic driving database were used for calibration purposes, a qualitative visualization of the data and the model fit is provide for single driver. Driver 316 was selected for the detailed analysis because the relative goodness of fit for each of the models was similar to the aggregate data results.

First-Order Model Results

The results of simulation using the Van Aerde first-order model are shown below, with TABLE 1 providing quantitative measures, and FIGURE 2 providing qualitative fits to the data. The results presented in TABLE 1 demonstrate a high level of variability in the model's ability to simulate different drivers, with the RMSPe value for driver 350 over six times that for driver 363, at 0.00105 and 0.00017, respectively. This could be attributed to the lower number of observations for driver 350.

The aggregate results entail the following parameters: a jam density (k_j) of 169 veh/km, resulting in a vehicle spacing at jam density of 5.9 meters; a flow-at-capacity (q_c) of 0.662 vehicles per second per lane, approximately equal to 2,400 vehicles per hour per lane; a speed-at-capacity of 22.83 m/s, around 82 km/h; and a desired speed or free-flow of 28.31 m/s, approximately equal to 102 km/h. These parameter values appear to be very reasonable.

TABLE 1 Results for the Van Aerde model

Parameter	D124	D304	D316	D350	D358	D363	D462	Aggregate
k_j^a (veh/m)	0.149	0.154	0.124	0.138	0.161	0.150	0.131	0.169
q_c^a (veh/s)	0.948	1.000	0.523	0.611	0.514	0.975	1.000	0.662
\dot{x}_c^a (m/s)	23.56	16.67	22.28	22.31	19.14	19.06	22.22	22.83
\dot{x}_d^a (m/s)	29.14	31.94	26.81	26.06	32.22	31.94	31.94	28.31
No. Obs.	47,623	41,819	114,211	39,625	110,938	105,573	14,645	474,434
RMSPe	0.00073	0.00037	0.00036	0.00105	0.00030	0.00017	0.00052	0.00018

^a denotes values optimized using SPD-CAL

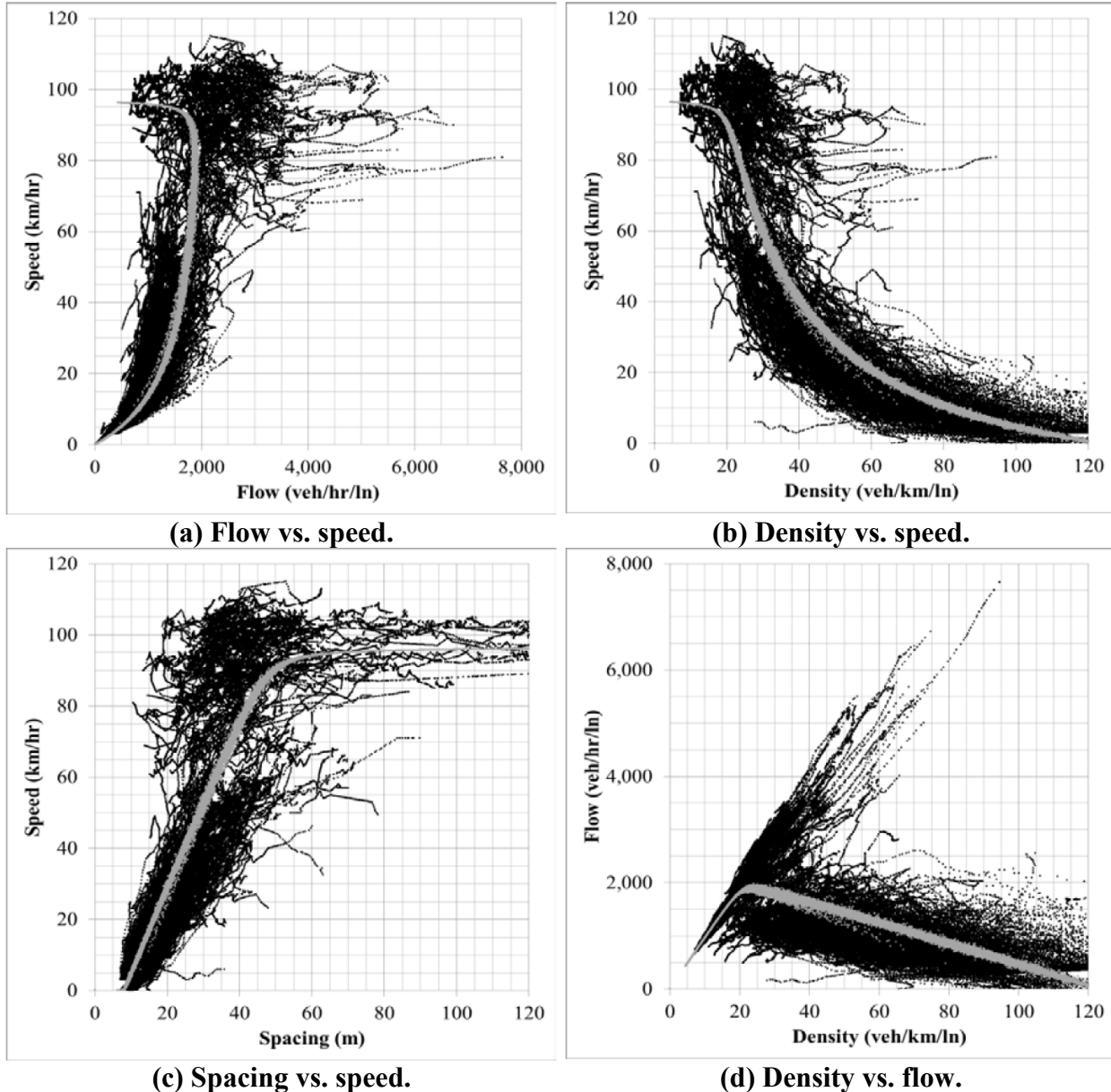


FIGURE 2 Driver 316 combined interaction diagram results for car-following simulation using Van Aerde model; displaying (a) flow vs. speed, (b) density vs. speed, (c) spacing vs. speed, and (d) density vs. flow.

Qualitatively, it is seen in FIGURE 2 that the steady-state Van Aerde model accurately captures the underlying average driver behavior, but fails to capture the variability that is seen in the driver behavior. Furthermore the model is unable to capture the inverted lambda shape associated with the speed-density data. This is because first-order models are unable to capture the capacity drop associated with discharging from congestion. It should be noted that it is possible to build in variability to the four calibrated parameters, but the behavior itself is influenced by additional factors outside of the scope of a first-order model. In the study herein variability in parameter values between trips for a given driver is inappropriate, as each individual trip may be biased in one direction or the other. Calibrating parameter values for

individual car-following events was explored, but found to yield inconsistent results due to the small dataset represented by each event.

RPA Second-order Model Results

The original formulation of the RPA model addresses some of the disparity seen between the simulated Van Aerde steady-state model and the observed behavior, by imposing a collision avoidance constraint and a vehicle dynamics constraint. The results of simulation for the RPA model are shown below, with TABLE 2 providing quantitative measures, and FIGURE 3 providing qualitative measures. Similar to the first-order model results, a high level of variability can be seen in the model's ability to simulate the driving behavior of each individual driver. Although the collision avoidance and vehicle dynamics constraints provide logical restrictions to the steady-state behavior predicted by the Van Aerde model alone, the measure of error is seen to increase slightly for both the individual drivers and the aggregate results. An argument could be made based on these quantitative results that the RPA second-order model should not be used, and instead the formulation using only the steady-state Van Aerde model is better, but it is necessary to analyze the qualitative results to determine if this is the case.

TABLE 2 Results for the RPA model

Parameter	D124	D304	D316	D350	D358	D363	D462	Aggregate	
k_j^a	0.149	0.154	0.124	0.138	0.161	0.150	0.131	0.169	
q_c^a	0.948	1.000	0.523	0.611	0.514	0.975	1.000	0.662	
\dot{x}_c^a	23.56	16.67	22.28	22.31	19.14	19.06	22.22	22.83	
\dot{x}_d^a	29.14	31.94	26.81	26.06	32.22	31.94	31.94	28.31	
\ddot{x}_{d-min}^b	-4.630	-2.778	-3.472	-5.556	-5.556	-4.861	-2.451	-4.481	
γ^b	0.631	0.600	0.710	0.537	0.576	0.529	0.639	0.764	
Vehicle	P^b	90	90	90	90	145	145	119	90
	$mass^b$	1190	1090	1090	1090	1375	1375	1900	1190
	C_d^b	0.36	0.40	0.40	0.40	0.40	0.40	0.50	0.36
	A_f^b	2.06	2.00	2.00	2.00	2.18	2.18	2.94	2.06
No. Obs.	47,623	41,819	114,211	39,625	110,938	105,573	14,645	474,434	
RMSPe	0.00086	0.00037	0.00044	0.00118	0.00034	0.00019	0.00087	0.00021	

^a denotes values optimized using SPD-CAL

^b denotes values observed from dataset

Noteworthy is that in the case of the RPA model the Van Aerde model parameters were held constant. These parameters included the jam density, the flow-at-capacity, the speed-at-capacity, and the desired speed or free-flow speed. These parameters are calibrated using steady-state observations only, as defined by accelerations ranging between plus and minus 0.5 m/s^2 . The desired minimum acceleration and maximum throttle level (γ) were obtained directly from the empirical data. The vehicle characteristics were obtained from manufacturer information based on the vehicle make, model, and year.

Qualitatively, as demonstrated in FIGURE 3, the RPA model provides better coverage of the observed driver behavior when compared to the first-order Van Aerde model (shown in FIGURE 2). Specifically, the average driver behavior defined by the steady-state formulation remains intact, while the collision avoidance constraint imposes departures from the steady-state behavior to maintain a safety buffer, and the acceleration constraints are observed to delay the return to the steady-state behavior when a vehicle accelerates. The breadth of driver behavior appears to

reflect the more conservative driving conditions; however the RPA model does not capture the more aggressive driving behavior adequately.

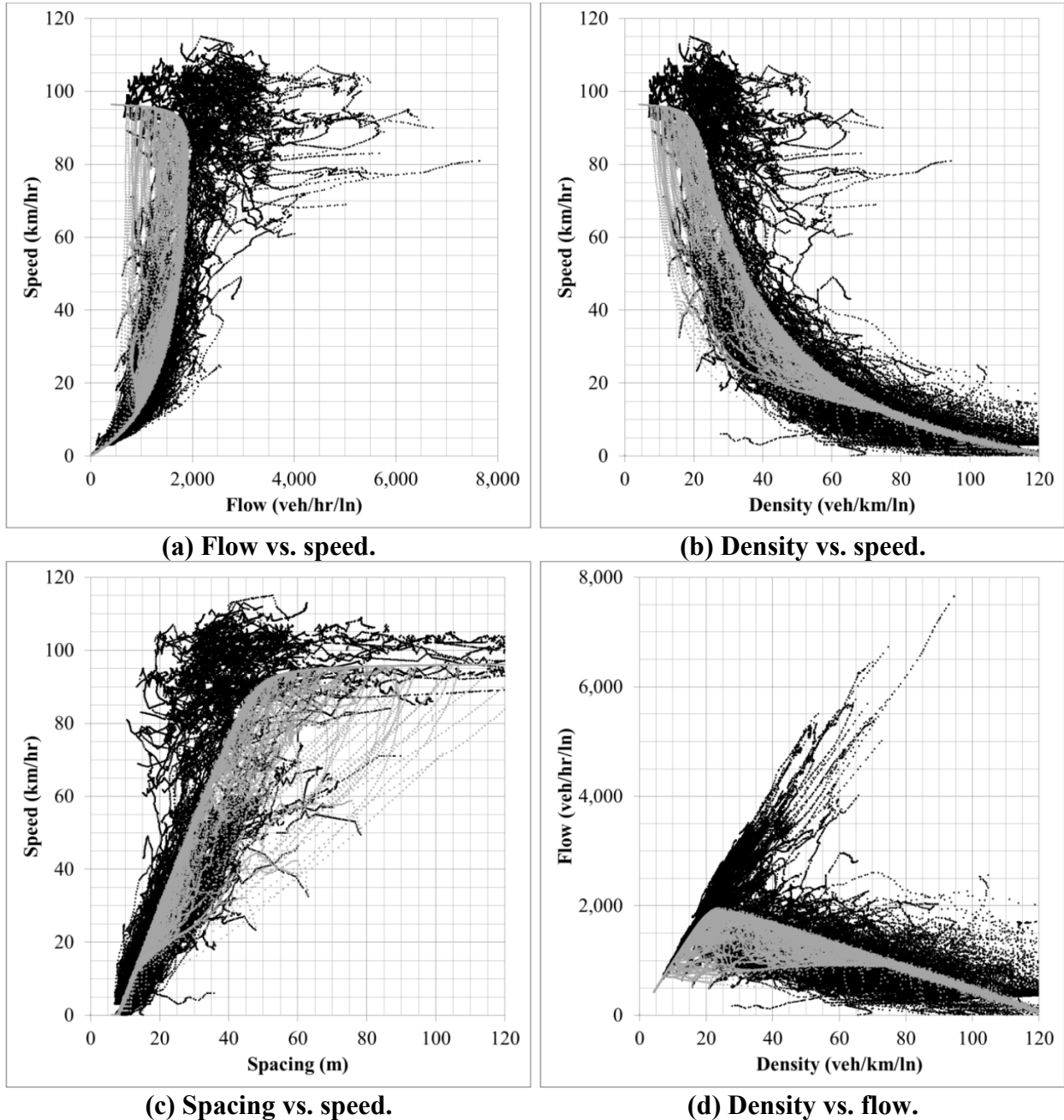


FIGURE 3 Driver 316 combined interaction diagram results for car-following simulation using original RPA model; displaying (a) flow vs. speed, (b) density vs. speed, (c) spacing vs. speed, and (d) density vs. flow.

Empirical Observations of Driver Behavior

The RPA second-order model appears to not capture empirical driver behavior associated with traveling at high speeds and very short vehicle spacing, as best seen in part (c) of FIGURES 1, 2,

and 3. Some of the individual car-following events exhibiting this behavior were further examined to determine if there was a consistent cause for the observed aggressive driving behavior. One observation was that a significant number of these events occurred when a vehicle in an adjacent lane entered the subject vehicle lane and forced the vehicle spacing to be very short.

The RPA model appeared to deviate from the empirical observations in two other ways: converging to a steady-state behavior at low velocities and displaying significantly more conservative driving behavior on some individual events.

The low-velocity convergence to steady-state conditions can be seen in parts (a), (b), and (c) of FIGURE 3, which all display speed on the y-axis. As speed decreases from 20 m/s to 10 m/s, the driver behavior converges to the steady-state behavior, in contrast to the variability displayed in the empirical data. The observed data aggregated across all seven drivers is displayed in FIGURE 1, with the darkness of each observation point showing the instantaneous velocity at that observation, with darker points indicating high acceleration and lighter points indicating high deceleration. By examining parts (a), (b), and (c) of this figure it is seen that the low-velocity regime yielding steady-state results in the simulation exhibits stark variation in driver behavior between acceleration and deceleration. Two methodologies are available to introduce hysteresis into the current model formulation, the first could be to calibrate separate values for the jam density parameter to be used in accelerating and decelerating behaviors, and the second could be to introduce a perception-reaction time-lag into the model.

The causes of the conservative driving behavior exhibited by the RPA model can be seen in the formulation of the additional constraints. Although the RPA model imposes a vehicle dynamics limitation on acceleration, it does not impose a similar limitation on deceleration. In a case where the observed car-following event begins with a high velocity and a short space headway, such as at a speed of 100 km/h and a space headway of 20 m, the simulated model will drive the instantaneous deceleration to be around -600 m/s^2 to arrive at a velocity of 40 km/h in the next time step, in keeping with the steady-state relationship predicted. So long as the lead vehicle is traveling at a greater speed than the following vehicle, such as, for example 101 km/h in the previous example, the collision avoidance constraint is not activated, and the steady-state component governs. In keeping with the ideals of the constraints added to the Van Aerde model to make up the RPA model, the authors herein sought to determine a constraint for deceleration based on physical mechanisms.

PROPOSED MODIFICATIONS TO THE MODEL

Initially, the authors herein postulated that a limitation on deceleration based on the maximum braking potential of a vehicle would improve the simulated model results, but it was found that this produced far more aggressive braking than was observed in the dataset. The naturalistic database included a parameter to record the relative depression of the brake pedal for each time step, but a review of the database showed that these values were null, so it was not possible to assign each driver a maximum desired braking factor. By conducting parameter calibration to minimize the error function, a desired deceleration value was calculated for each driver, to govern his/her behavior in aggressive driving situations not being overruled by the collision avoidance constraint. The authors found that the drivers desired to decelerate at relatively gentle rates, even when inhabiting more aggressive parts of the interaction diagram than was desired. Upon further review, it was found that the desired rate of deceleration for each driver was very close to the deceleration imparted by the combined resistance forces of the vehicle dynamics model, essentially implying that the observed behavior of drivers is to coast, using neither the

gas nor the brake pedals, gradually backing off of a lead vehicle when the space headway is smaller than it is wished to be for a given speed. Subsequently, the authors herein propose an additional constraint to the existing RPA model for use with deceleration behavior not governed by the collision avoidance constraint. We recommend using the vehicle dynamics constraint with the throttle, herein defined as γ , set to zero, which allows the simulated vehicle to coast out of aggressive driving conditions until it reaches its desired steady-state behavior.

At this time, the jam density parameter is not being modeled with separate values for the case of acceleration and deceleration, despite the indication from the observed data that this may improve the accuracy of the simulated results. A trial of this model variation was conducted, and while it resulted in an improvement to the qualitative results on the interaction diagram, there was no change to the quantitative error measure. In order to introduce hysteresis into the simulation results, a perception-reaction component has been added to the model, basing simulated following driver behavior on observed leading driver behavior occurring τ seconds in the past. Staying internally consistent with the components of the model, the value of τ is set equal to the value of the c_3 parameter calculated for the first-order steady-state model.

Use of Vehicle Dynamics for Coasting

Incorporating the proposed condition of vehicle coasting in aggressive driving conditions when the collision avoidance constraint is not triggered, the components of the RPA model, being represented by Equations (3), (4), and (5) are implemented in the proposed modified formulation as shown in Equation (9).

$$\dot{x}_{n+1}(t) = \max[\min(\dot{x}_{n+1}^{(2)}, \dot{x}_{n+1}^{(3)}(\gamma = 0)), \min(\dot{x}_{n+1}^{(1)}, \dot{x}_{n+1}^{(2)}, \dot{x}_{n+1}^{(3)})] \quad (9)$$

Results of the Modified RPA Model

The modified formulation of the RPA model addresses most of the disparity seen between the simulated Van Aerde steady-state model behavior and the observed behavior, qualitatively covering the aggressive driving conditions observed in the database that were not being incorporated by either the Van Aerde model or the existing formulation of the RPA model. The results of simulation for the modified RPA model are shown below, with TABLE 3 providing quantitative measures, and FIGURE 4 providing qualitative measures. The results of the error measure are seen to improve with the modifications to the RPA model, with further comparative analysis offered below. The qualitative results show improvements in keeping with the benefits seen in the quantitative results.

This modified model is an expansion of the regimes of behavior from the previous formulation using the same set of equations, and not an alternative way to calibrate the behavior. As such, the modified formulation of the driver behavior model uses the same set of calibrated parameters as the original formulation.

TABLE 3 Results for the modified Rakha-Pasumarthy-Adjerid model

Parameter	D124	D304	D316	D350	D358	D363	D462	Aggregate	
k_j^a	0.149	0.154	0.124	0.138	0.161	0.150	0.131	0.169	
q_c^a	0.948	1.000	0.523	0.611	0.514	0.975	1.000	0.662	
\dot{x}_c^a	23.56	16.67	22.28	22.31	19.14	19.06	22.22	22.83	
\dot{x}_d^a	29.14	31.94	26.81	26.06	32.22	31.94	31.94	28.31	
τ^a	0.7	0.3	1.5	1.3	1.4	0.4	0.5	1.2	
\ddot{x}_{d-min}^b	-4.630	-2.778	-3.472	-5.556	-5.556	-4.861	-2.451	-4.481	
γ^b	0.631	0.600	0.710	0.537	0.576	0.529	0.639	0.764	
Vehicle	P^b	90	90	90	90	145	145	119	90
	$mass^b$	1190	1090	1090	1090	1375	1375	1900	1190
	C_d^b	0.36	0.40	0.40	0.40	0.40	0.40	0.50	0.36
	A_f^b	2.06	2.00	2.00	2.00	2.18	2.18	2.94	2.06
No. Obs.	46,495	41,511	109,563	36,397	105,179	104,751	13,981	455,382	
RMSPe	0.00065	0.00032	0.00029	0.00088	0.00029	0.00015	0.00036	0.00015	

^a denotes values optimized using SPD-CAL

^b denotes values observed from dataset

Qualitatively, it is seen in FIGURE 4 that the modified RPA model provides better coverage of the observed driver behavior than does either of the previous two versions of the model, shown in FIGURE 2 and FIGURE 3. Specifically, the centroid behavior defined by the steady-state formulation remains in the same location, while the collision avoidance constraints impose departures from this curve to maintain safety, the acceleration constraints slow the return to the steady-state behavior once the collision avoidance condition has been met, the coasting constraint allows for gradual deceleration when traveling in an aggressive traffic stream, and finally the perception-reaction time delay introduces hysteresis at low velocities. Additionally, in the case of the specific driver displayed in the interaction diagram the model appears to miss a segment of less aggressive driving behavior in the range of twenty kilometers per hour to 60 kilometers per hour. This may or may not be due to factors impacting the driver's behavior which are not observed herein, such as traffic behavior upstream of the driver, inclement weather, glare, etc.

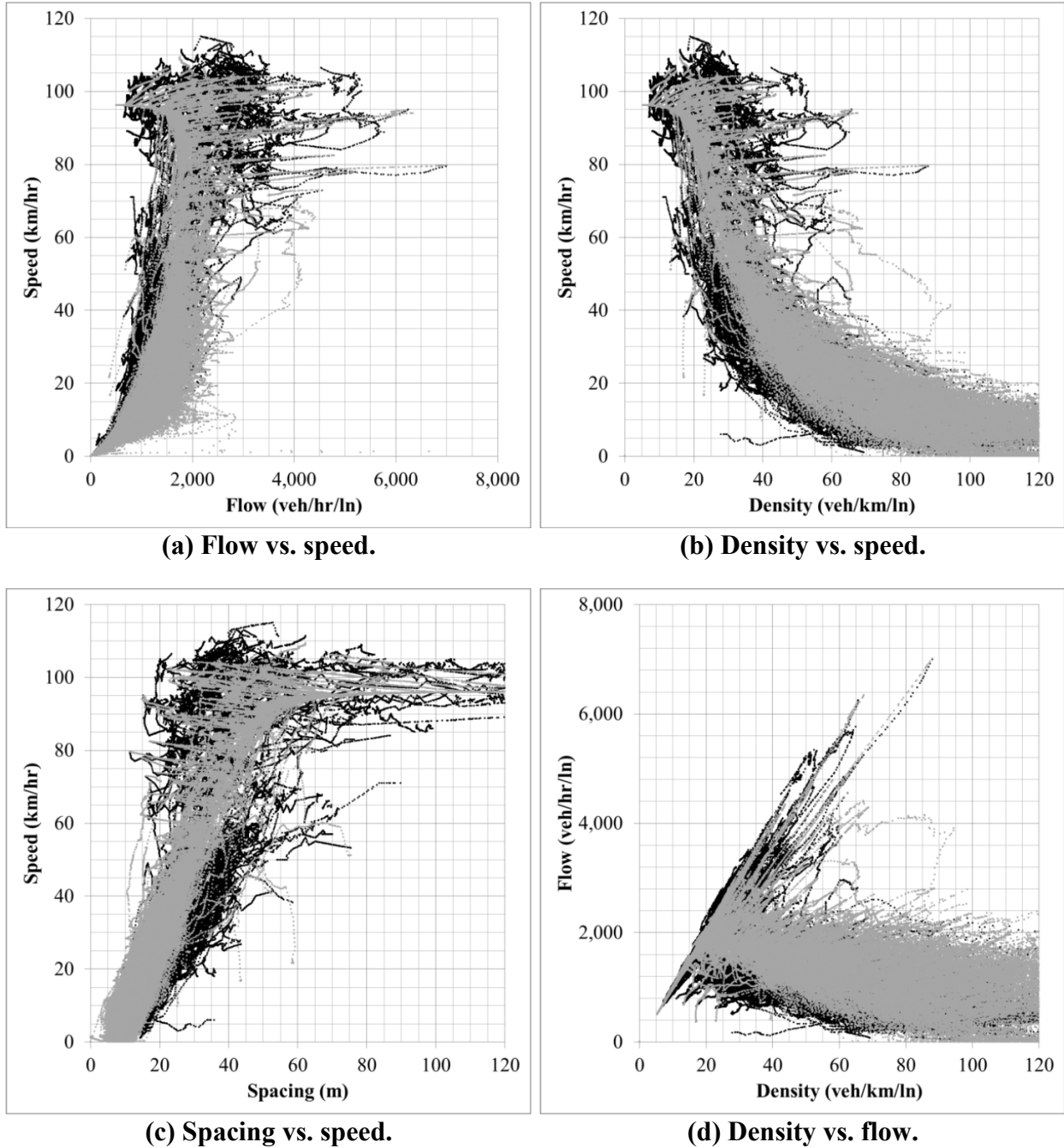


FIGURE 4 Driver 316 combined interaction diagram results for car-following simulation using modified RPA model; displaying (a) flow vs. speed, (b) density vs. speed, (c) spacing vs. speed, and (d) density vs. flow.

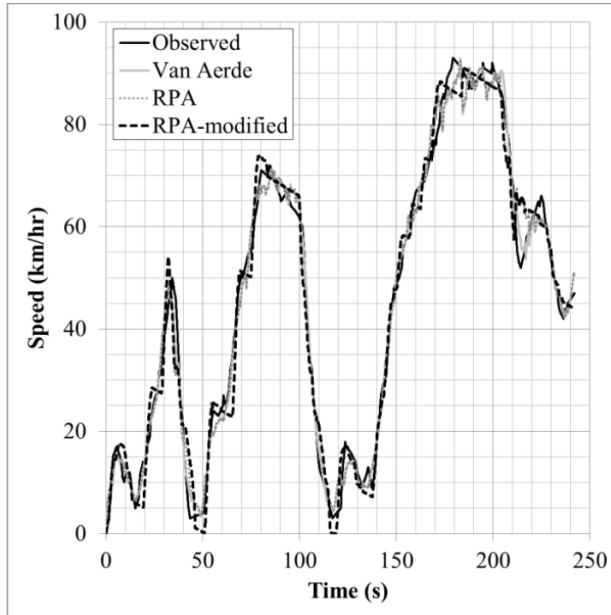
COMPARATIVE ANALYSIS FOR MODEL FORMULATIONS

The comparative error results of simulation for the Van Aerde model, the original RPA model, and the modified RPA model are shown in TABLE 4. Because of the amount of overlap between the three models, qualitative comparison is provided through the use of sample car-following events, with time vs. speed and time vs. spacing charts provided for two individual events in FIGURE 5. The results of the error measure is seen to decrease universally with the

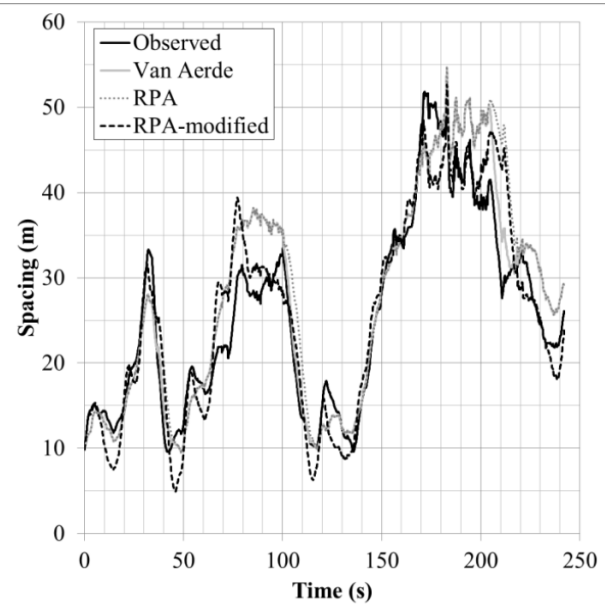
modifications to the model, but for the individual drivers and in the aggregate results; the modified RPA model has an RMSPE which is 20% lower than the Van Aerde model, and 40% lower than the original formulation of the RPA model.

TABLE 4 Comparative error results

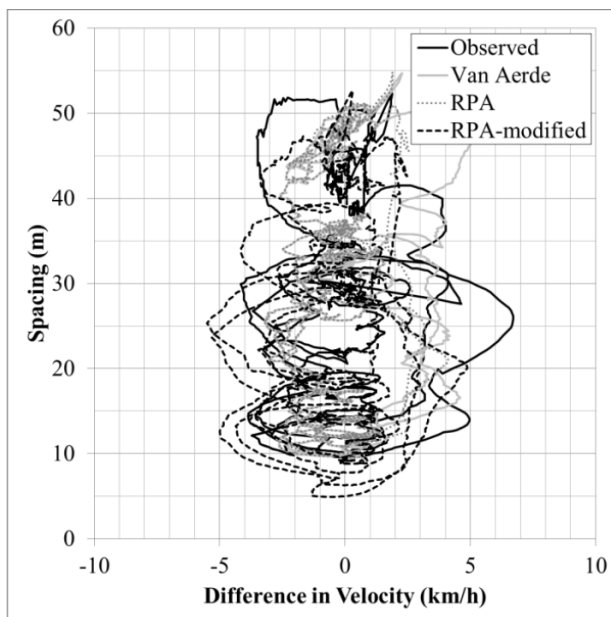
Model	D124	D304	D316	D350	D358	D363	D462	Aggregate
Van Aerde	0.00073	0.00037	0.00036	0.00105	0.00030	0.00017	0.00052	0.00018
RPA	0.00086	0.00037	0.00044	0.00118	0.00034	0.00019	0.00087	0.00021
RPA-modified	0.00065	0.00032	0.00029	0.00088	0.00029	0.00015	0.00036	0.00015



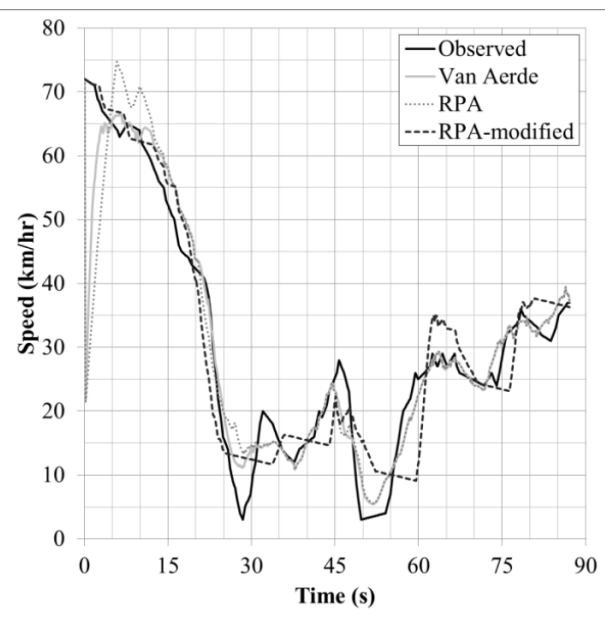
(a) Time vs. speed, event 21958.09.



(b) Time vs. spacing, event 21958.09.



(c) Speed vs. velocity diff., event 21958.09.



(d) Time vs. speed, event 90700.01.

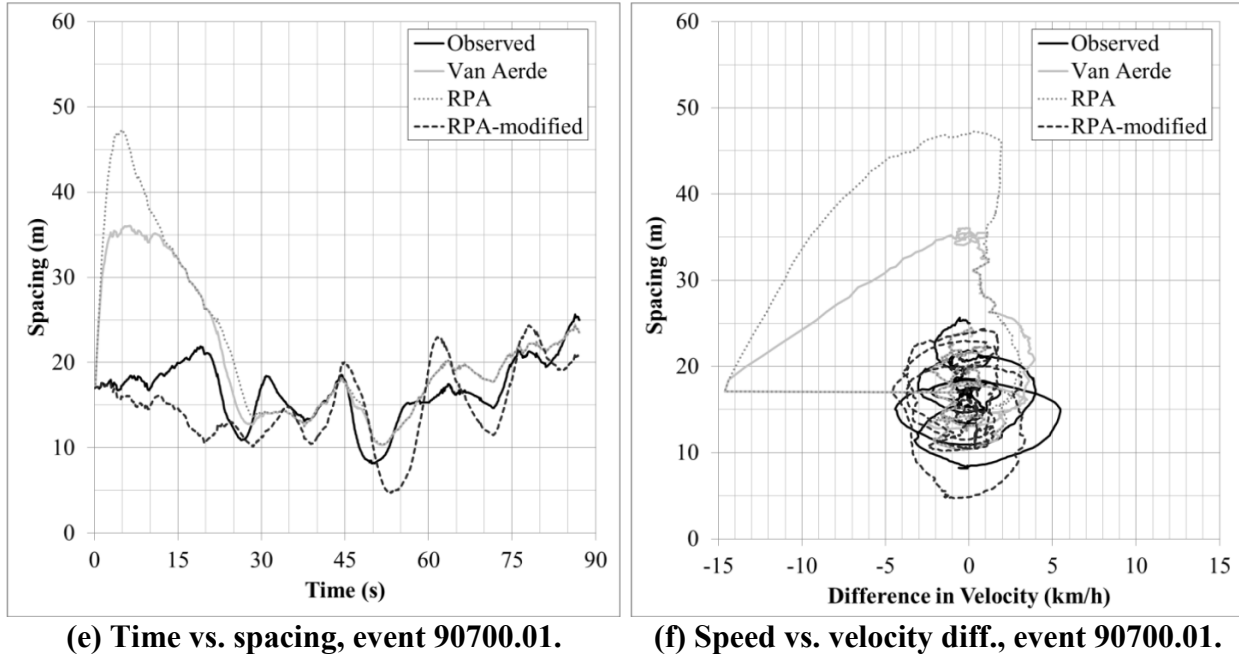


FIGURE 5 Sample car-following events: event 21958.09 (a) time-speed diagram, (b) time-spacing diagram, and (c) spacing-velocity difference diagram; event 90700.01 (d) time-speed diagram, (e) time-spacing diagram, and (f) spacing-velocity difference diagram.

The individual car-following events displayed in FIGURE 5 serve to highlight both the logical errors found from the original formulation of the RPA model, and show how a specific dataset can lead to an oversight. Naturalistic driving data includes vast stores of data from many drivers as they go about their regular driving activities, using vehicles which have been equipped to record their travel data without interfering with regular operations. If the data used in this current study had included only test-track data, or if it had included only data observed along arterials, it is possible that every car-following event would have begun at a very low speed, such as is seen in parts (a), (b), and (c) of FIGURE 5; in this case the modified formulation of the RPA model is seen qualitatively to work as well as either the original formulation of the RPA model or the Van Aerde model. It is only because the naturalistic data used for analysis herein includes travel on a multi-lane highway that car-following events can begin with lead vehicles entering the lane in front of an instrumented vehicle at high velocity. The second example car-following event, shown in parts (d), (e), and (f) of FIGURE 5, displays the improvement provided by the modified RPA model, in comparison to the Van Aerde model and original formulation of the RPA model, specifically in the case of car-following events beginning at high-speed and high-density. The instantaneous deceleration discussed previously is clearly seen here, along with the resulting jump in spacing between the lead and follower vehicle for the first segment of the event. Of interest, the error appears to be self-regulating, as the spacing of the follower vehicle for all three variations of the model formulation are consistent after the initial thirty seconds of the event.

Speed-spacing Area for Observed Data and Simulated Data

In an effort to measure both the quantitative and qualitative dispersion of the observed and simulated data on the interaction diagram, a methodology was developed to look at area

coverage in a true/false sense between the observed driver behavior and the simulated driver behavior. An initial effort was made to perform analysis using probability distribution functions, but it was found that there was either too much variability, or too little data points for central tendencies and distribution shapes to be identified.

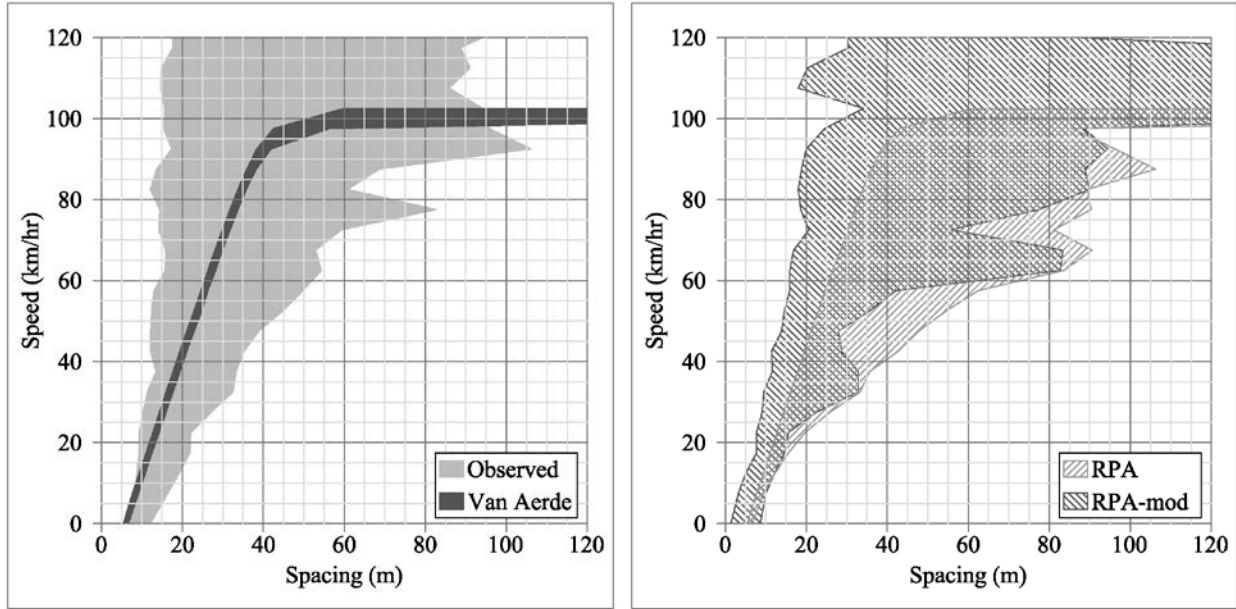
Using the spacing versus speed charts from the interaction diagram, as seen in part (c) of FIGURES 1, 2, 3, and 4, a procedure was developed to identify the breadth of the data without including outlier information, for comparison purposes. Data points were first separated into bins based on velocity, with a bin size of five kilometers per hour. With the points defined for a given speed bin, the 5th and 95th percentile values were calculated. The shape of the distributed data was plotted using a Computer Aided Drafting program, with calculations conducted regarding the area of overlap between the observed data and the simulated results.

The results of the dispersion analysis are shown quantitatively in TABLE 5, and qualitatively in FIGURE 6. It was found that the Van Aerde model coverage included 7 percent of the observed dataset, the true-true result; with 19 percent of the simulated data appearing outside of the area of observed data, a false-true result. In covering the observed data, the original RPA formulation improved the true-true result to 40 percent, with the modified model improving the result to 71 percent. The data point distribution as generated by either version of the RPA model is about equal, with a false-true result of 40 percent and 39 percent for the original and modified models, respectively.

In general, the qualitative data distribution shown in FIGURE 6 sums up the information previously discussed; the Van Aerde model generates a thin stream of simulated data along the centroid of the observed data, the original RPA model generates data that is equal to or more conservative than the steady-state behavior, and the modified RPA model includes more aggressive driving behavior as a driver chooses to coast from more aggressive to steady-state driving conditions.

TABLE 5 Coverage of the middle 90th percentile of simulated and observed data

Speed-Spacing Area (m-km/hr) 5th to 95th percentile		D124	D304	D316	D350	D358	D363	D462	Aggregate
Observed Area		4,575	4,076	3,846	3,945	3,762	3,774	1,888	5,985
Van Aerde	Simulated Area	135	769	786	2,086	538	557	387	1,519
	True-True	3%	11%	13%	9%	9%	10%	19%	7%
	False-True	0%	7%	7%	44%	5%	5%	2%	19%
RPA	Simulated Area	3,345	3,704	2,162	5,083	1,866	2,590	2,489	4,681
	True-True	58%	62%	39%	50%	34%	53%	46%	39%
	False-True	15%	29%	17%	79%	16%	16%	86%	39%
RPA- mod	Simulated Area	5,220	4,953	2,656	5,108	2,914	3,044	1,678	6,138
	True-True	78%	83%	61%	72%	67%	68%	66%	67%
	False-True	36%	38%	9%	57%	10%	13%	23%	35%



(a) Observed and Van Aerde results.

(b) RPA and RPA-modified results.

FIGURE 6 Coverage of the middle 90th percentile of simulated and observed data, displaying (a) observed and Van Aerde data, and (b) RPA and the modified RPA results.

CONCLUSIONS

This paper analyzed the simplified behavioral vehicle longitudinal motion model, currently integrated in the INTEGRATION software, which has been named the Rakha-Pasumarthy-Adjerid model in the literature. The current model utilizes a steady-state model along with two constraints, acceleration and collision avoidance. A naturalistic driving database, the Hundred Car Study, was used to generate 1,732 car following events totaling 789 minutes worth of data across seven drivers, along the same stretch of multi-lane highway.

Based on analysis of the current model using this unique data set, a deficiency was identified in the current formulation of the model in that it predicts more conservative driving behavior than is observed. Although the simulated data produced by the existing RPA model provides qualitative results that improve upon the steady-state Van Aerde model, there is increased error in the quantitative results. Further comparative review indicated that much of the error occurs when a car-following event is initiated, specifically when an event begins while both vehicles are traveling at high speeds. As a leading vehicle enters the travel-way in front of a given probe vehicle, the spacing between the two vehicles is often much shorter than is desired when traveling at high speed. The existing models do not constrain for deceleration behavior, and the simulated behavior was found to match the desired speed based on the observed space headway. This was observed to result in near-instantaneous deceleration.

When an overly aggressive speed versus space headway is imposed on a following vehicle at the beginning of a car-following event, the observed behavior is that, rather than decelerating swiftly, the following vehicle instead chooses to coast until the desired headway is achieved. A modification to the existing model, using the vehicle dynamics equations was proposed to incorporate this observed behavior. Quantitative and qualitative analysis comparing the previous and the proposed model formulations shows that this modification provides significant benefit to the results.

The proposed modifications are found to significantly decrease the error against the observed behavior in comparison to either of the two previous formulations, reducing error in the aggregate case by 20 percent against the Van Aerde model, and by 40 percent against the original RPA formulation. Additional qualitative analysis using both time-space and time-speed diagrams of individual trips, and using data distribution diagrams, indicates that the proposed modifications to the RPA model result in a more realistic simulation of driver behavior.

ACKNOWLEDGEMENT

The authors acknowledge the financial support provided by the FHWA and the Mid-Atlantic University Transportation Center (MAUTC) in conducting this research effort.

REFERENCES

- [1] S. Panwai and H. Dia, "Comparative Evaluation of Microscopic Car-Following Behavior," *IEEE Transactions on Intelligent Transportation Systems*, vol. 6, no. 3, pp. 314-325, Sep. 2005.
- [2] T. Kim, D. Lovell, and Y. Park, "Limitations of Previous Models on Car-Following Behavior and Research Needs," in *Transportation Research Board, 82nd Annual Meeting of the*, 2003, no. 03.
- [3] M. Van Aerde and H. A. Rakha, "Multivariate Calibration of Single Regime Speed-Flow-Density Relationships," *Vehicle Navigation and Information Systems, Proceedings of the 6th International Conference on*, pp. 334-341, 1995.
- [4] H. A. Rakha, P. Pasumarthy, and S. Adjerid, "A simplified behavioral vehicle longitudinal motion model," *Transportation Letters: The International Journal of Transportation Research*, vol. 1, no. 2, pp. 95-110, 2009.
- [5] S. Park, H. A. Rakha, R. Alfelor, C. Y. D. Yang, and D. Krechmer, "Empirical Study of Impact of Icy Roadway Surface Condition on Driver Car-Following Behavior," in *Transportation Research Board, 90th Annual Meeting of the*, 2011, vol. 982, no. 617.
- [6] H. A. Rakha, M. Snare, and F. Dion, "Vehicle Dynamics Model for Estimating Maximum Light-Duty Vehicle Acceleration Levels," *Transportation Research Record: Journal of the Transportation Research Board*, vol. 1883, pp. 40-49, Jan. 2004.
- [7] H. A. Rakha and M. Arafeh, "Calibrating Steady-State Traffic Stream and Car-Following Models Using Loop Detector Data," *Transportation Science*, vol. 44, no. 2, pp. 151-168, Dec. 2010.